750

S-319

NASA CR-66261

LASER NOISE: THEORY AND EXPERIMENT

FINAL REPORT

Contract No. NAS 1-6003

nes

25 November 1966

NATIONAL ENGINEERING SCIENCE CO.

Prepared for

Langley Research Center
National Aeronautics Space Administration
Hampton, Virginia

PRECEDING PAGE BLANK NOT FILMED.

NASA CR-66261

FINAL REPORT

LASER NOISE: THEORY AND EXPERIMENT

Prepared for

Langley Research Center
National Aeronautics Space Administration
Hampton, Virginia

Prepared by

H. Hodara
N. George
J. Yoh

NASA Contract Report No. 66261

Contract No. NAS 1-6003

25 November 1966

NESCO Report No. S-319

NATIONAL ENGINEERING SCIENCE COMPANY
711 South Fair Oaks Avenue
Pasadena, California 91105

PRECEDING PAGE BLANK NOT FILMED.

ACKNOWLEDGEMENTS

We would like to thank Duncan McIver and John Randolph from NASA for valuable discussions. Further, we would like to acknowledge that portions of this work were carried out at the Quantum Electronics Laboratory of the California Institute of Technology under contract support of the Air Force Office of Scientific Research.

This report and the experiments whose results are illustrated in Figs. 4 to 12 were done by the authors during the period extending from September 1, 1966 to November 18, 1966.

PRECEDING PAGE BLANK NOT FILMED.

ABSTRACT

Two major noise sources have been identified in dc discharge gas lasers: plasma noise and multimode noise. These sources may lead to a 20- to 30-db increase in noise above the shot noise level in certain bands of the spectrum extending from a few KHz to several MHz. This increase in noise can degrade the performance of an optical communications system. The presence of these noise sources, the spectral location, and the magnitude for several helium-neon lasers investigated is the subject of this report. Experimental results reveal that plasma noise can be reduced by increasing the filament current in the laser tube, and multimode noise can be controlled by inserting an iris in the laser cavity to eliminate off-axis modes. Careful choice of mirror separation and curvature also helps to minimize low frequency noise.

PRECEDING PAGE BLANK NOT FILMED.

CONTENTS

1. INTRODUCTION

The random fluctuations in the photodetected current from a laser constitute noise. These fluctuations, appearing at the detector output as intensity fluctuations, are caused by amplitude as well as phase variations of the laser field. Although their sources are many, we have concentrated on measuring the ones inherent to the laser itself. We have found two major noise contributions in dc discharge gas lasers: plasma noise and multimode noise. Each one may be responsible for as much as 20 to 30 db of noise in certain bands of the spectrum extending from a few kHz to several MHz (Ref. 1). This noise degrades the performance of communications systems by several decibels; it also introduces errors in propagation measurements as these fluctuations often exceed those created by atmospheric turbulences.

The presence of these noise sources, their spectral location, and their magnitude is the subject of this investigation. Resultants of this work are guidelines and criteria of laser design aimed at reducing or eliminating these additional sources of noise.

2. RESULTS

Plasma noise in dc discharges of HeNe lasers operating at 6328Å has been eliminated by increasing the filament current in the laser tube. The random oscillations disappear completely in the range 0.1 to 100 kHz. However, no measurements were made beyond 100 kHz to determine if oscillations appeared at higher frequencies. A tentative explanation for the disappearance of these oscillations is given in Section 3.

Multimode noise can be controlled, with consequent output reduction, by inserting an iris in the laser cavity and cutting down the beam diameter to the point where off-axis modes are sharply reduced. Alternatively, low frequency noise in the kHz range can be minimized by choosing the mirror separation and curvature so that higher order transverse modes are spaced by several MHz, i.e., several natural linewidths from the dominant TEM_{qoo} modes; this greatly decreases mode competition interactions and thereby lessens the amount of noise in the low frequency (LF) portions of the photodetected current.

3. PLASMA NOISE

3.1 Experiment

The experimental setup appears in Fig. 1a. Photographs are shown in Fig. 1b. The discharge current fluctuations are monitored spectrally on the 1 to 100 kHz analyzer; the incoherent light from the discharge is detected via photomultiplier No. 1 and the laser light via photomultiplier No. 2. Both photomultiplier outputs are analyzed for spectral fluctuations on an LF wave analyzer covering the band 100 Hz to 50 kHz.

The major result of the experiment is illustrated in Figs. 2 a through 2c. The plasma exhibits low frequency oscillations around 19 kHz which show up in the spectrum of the discharge current I_L (Fig. 2a). These fluctuations also show up in the incoherent or side light from the laser tube (Fig. 2b) which is attributed to the fact that these fluctuations are caused by "moving striations" in the plasma (Ref. 2). The gain of the tube is modulated accordingly by these oscillations since the laser output current I_{pm} also exhibits peak fluctuations at the same frequency (Fig. 2c). We see then that striation oscillations around 19 kHz increase the laser noise output (Fig. 2c) by as much as 20 db. The slowly decaying noise spectrum between 12 and 19 kHz in the photocurrent of Fig. 2c is attributable to additional noise caused by random frequency modulation, i.e., instabilities in the plasma oscillation frequency (Ref. 3). These oscillations do not always occur at the same frequency for the same laser. Peak fluctuations occurring at 18 kHz and reaching a level 30 db above shot noise are shown in Fig. 3.

Another laser whose dimensions are shown in Fig. 1a was also investigated. The discharge current oscillations occur at 10 kHz with strong harmonics up to the fifth (Fig. 4a). Corresponding fluctuations show up in the laser output current (Fig. 4b). The laser was made to operate in locked modes as shown in Fig. 4b, which displays a single beat at 250MHz. The same laser, under identical operating conditions except for the fact that the modes are unlocked, is seen, (Figs. 5a and 5b) to have perfect correlation between the discharge current (Fig. 5a) and photocurrent fluctuations (Fig. 5b). Note the increase in photocurrent noise level due to the unlocked modes whose beats are displayed in Fig. 5b.

The strong dependence of striation oscillations on filament current is positively confirmed by the results shown in Figs. 6a through 6ℓ and 7a through 7h. Figure 6b shows that with higher filament current (rheostat setting = 57)*, striation oscillations do not take place until the discharge laser current I_L reaches 9.5 ma. The fundamental oscillation is around 25 kHz with harmonics showing up as I_L increases (Figs. 6a to 6ℓ). At lower filament currents (rheostat setting = 55)* oscillations begin to show up for discharge current of I_L = 4.5 ma (Fig. 7b) at about the same frequency and increase in strength with strong harmonic dependence as the discharge current increases. No specific relation appears between current and oscillation frequency; there is a strong probability that the observed frequency shifts are caused by plasma instabilities.

3.2 Physical Interpretation

From the data presented in the previous section, it is clear that the oscillations in the dc current of the plasma column of a few percent are also evident as modulation of the coherent output of the laser. These modulated optical modes are not separately resolved in a scanning interferometer display and while they are evident in the photodetected output tuned to the dominant mode spacing $c/2L$,

*Rheostat settings are related to filament current as follows: setting 55 = 4.1 amperes; setting 57 = 4.2 amperes these beats have often been erroneously interpreted as frequency-pulled dominant mode beats of several longitudinal oscillations (the frequency spacing of 20 kHz is much too high for this effect with the 6328 Å laser).

From the low frequency spectral mode display, it is clear that each optical mode is modulated, and that optical sidebands are generated by these plasma oscillations. This effect was observed, in fact, independently by others and correctly interpreted as being due to plasma striations in the positive discharge column (Refs. 4 and 5). However, the suppression of these oscillations by simply increasing the space charge available at the cathode is reported for the first time in this report. Other more sophisticated methods of suppressing these oscillations would be the use of additional grids or partial rf excitation (Ref. 6).

Among the well-known types of oscillations in low-pressure dc discharges are the following (Ref. 7):

a) Striations

b) Ion acoustic

c) Electron plasma frequency

Extensive theoretical treatment of the striation phenomena has been made by Robertson (Ref. 8) and by Wojaczek (Ref. 9), and lengthy experimental treatises of note are those of Donahue and Dieke (Ref. 2), and Pekárek (Ref. 10). Briefly, it has been found that dc discharges in inert gases are almost always accompanied by moving or standing striations. These striations are thin annular discs along the positive column for which the electron concentration and temperature and the spontaneously emitted light are alternating in value. Modulation of the current is typically only a few percent; but the emitted light is deeply modulated, often dropping nearly to zero from a bright disc to a dark one.

Hakeem and Robertson have shown the important influence of the metastable levels of the inert gas atoms in striating a discharge column, and they predicted and later observed that there would not be any striations in discharges of alkali vapors, since these elements do not have neutral atom metastable states (Ref. 13).

It is relatively easy to explain the modulation of the optical modes in a qualitative way. First, it is important to clearly see that a striation is set up in the population density of the metastable neon atoms. As electrons in the discharge reach the negative glow, they get trapped; the resultant decline of current tends to extinguish the discharge. As the current decreases, the voltage increases, thus giving additional energy to the electrons that were traveling in the plasma column between the negative glow and the anode. These electrons have enough energy to ionize metastable Ne atoms by collisions with the resultant generation of a positive space charge which starts traveling toward the cathode. This traveling space charge constitutes a moving striation which, as it approaches the cathode, releases the trapped electrons in the negative glow. The whole process then repeats itself in a periodic fashion. It has been established that the speed of these striations depends on the lifetime of the Ne metastable atoms.

The short-lived $3s_2$ and $2p_4$ levels of neon are the upper and lower levels, respectively, for the laser transition at 6328 Å. The $2p_4$ level subsequently decays to the metastable Ne(1s), and it is this latter level which is striated in the positive column. For a higher population of Ne(1s), the deleterious repopulation of the Ne($2p_4$) by collisions with electrons of 3 volts or more energy can be expected to decrease the population inversion. Thus, the striations in the metastable Ne(1s) give rise to time-varying spatial modulation of the population inversion, and hence each optical mode is modulated.

It is also reasonable to conclude that the 1.15-μ laser transition ($2s_2$ to $2p_4$) will be similarly modulated since the same terminal level is involved. On the other hand, the 3.39-μ transition for the helium-neon laser ($3s_2$ to $3p_4$) is not as severely coupled to the Ne(1s) metastable level, and, therefore, the striation modulation of this laser line would be expected to be somewhat less.

Both the electron plasma frequency and the ion-acoustic phenomena are approximately independent of the tube radius, and the electron plasma frequency for the discharge parameters of the laser tube under consideration is approximately 4×10^9 Hz which is certainly well above the striation frequencies.

4. MULTIMODE NOISE

4.1 Experiment

The experimental setup is shown in Figs. 1a and 1b. An important feature of this experiment is a piezoelectric (PZT) crystal driving the curved mirror of the laser cavity. This allows changing the laser modes that can be excited in the cavity. Two different operations are possible. In the first, the PZT bias is varied manually while the mode change is observed both on the scanning interferometer oscilloscope display and on the RF spectrum analyzer via beats. In the other operation, the bias is adjusted at some value corresponding to a convenient cavity length and the PZT is driven by an audio oscillator at rates of the order of 0. 1 to 10 Hz. In both of these operations, the change in noise level is recorded on the Low Frequency (LF) Analyzer as a function of frequency. This is very well illustrated by the scanning interferometer displays of Figs. 8a through 8c, the RF beat display of Figs. 9a through 9c and the LF noise spectrum record of Fig. 10. This series of photographs in conjunction with the LF spectrum of Fig. 10 definitely proves that multimode operation is very noisy if the modes are unlocked. The scanning display of Figs. 8a through 8b indicates the presence of three longitudinal modes. The spacing between these modes is 250 mHz, corresponding to c/2L for the cavity. The sequence of Figs. 8a, 8b, and 8c brings out the effects of off-axis modes under locked (Fig. 8b) and unlocked condition (Fig. 8c). The off-axis modes 30 kHz apart are too close to be resolved by the scanning interferometer. Their presence, however, blurs, widens, and reduces the on-axis modes as seen in Fig. 8c. This is confirmed by the beats between off-axis and on-axis modes displayed on the RF spectrum of Figs. 9a, 9b, and 9c. The spacing is still 30 kHz; as the modes unlock from a to c in Fig. 9a, there is a one-to-one correspondence with the displays in Figs. 8a to 8c. In addition, a one-to-one correspondence also shows up in the low frequency noise recording of Fig. 10.

In this figure, the levels indicated by a, b, and c correspond to the equivalent labelings of Figs. 8 and 9. During these experiments, the unlocking was brought about by varying the PZT bias, and the discharge current fluctuations were checked to ensure that no plasma oscillations were present. The experiment was also repeated by keeping the PZT bias fixed and driving the crystal at 1 Hz rate. This unlocks and locks the modes at this rate with a corresponding increase and decrease in low frequency noise. The noise spectrum in Fig. 11 illustrates a case in point; the periodic change in noise level with PZT oscillation in the range 10 to 14 kHz, occurs at 1 Hz rate. The change in noise level in this case is of the order of 15 db.

4.2 Physical Interpretation

A preliminary theory of multimode noise has been published by the writers (Ref. 1) and will not be repeated here. A reprint of this reference is included in the Appendix for convenience. It is worth discussing how beats between on- and off-axis modes occur at frequency spacings of the order of 30 kHz. The cavity geometry for the laser of Fig. 1a is shown in Fig. 12a. It is nearly semiconfocal and the various order modes m, n (transverse), q (longitudinal) occur at frequencies (Ref. 11)

$$\nu_{mnq} = \frac{c}{2d}\left\{q + \frac{1}{2\pi}(1 + m + n)\cos^{-1}\left(1 - \frac{2d}{b}\right)\right\} \quad (5)$$

For the complete degenerate case (Fig. 12b) $d = b/2 = 60$ cm. A plot of the on-axis modes of order q and q-1 and off-axis modes q-1, m, n shows that the $(m + n) = 4$ order transverse mode pertaining to q-1 coincides with the q order on-axis mode. This is called, as we said, the complete degenerate case. If the cavity length is slightly perturbed from this dimension, the $(m + n) = 4$ order transverse mode pertaining to the q-1 on-axis modes may fall within a few kHz from the q- on-axis mode. The laser medium is capable of sustaining these two adjacent modes; mode competition results, giving rise to locking and unlocking with a corresponding change in low frequency noise levels. Saturating effects in the medium play an important role in this type of mode competition (Ref. 12). In the nondegenerate case, $2d/b \neq 1$, but close to unity. We define the parameter

$$\delta = 1 - \frac{2d}{b} \tag{6}$$

which is close to zero and find that the spacing between the first transverse mode and its corresponding on-axis mode is given by

$$\nu_{00q} - \nu_{01q} = \frac{c}{2d} \frac{\cos^{-1}\delta}{2\pi} \tag{7}$$

For $\delta \neq 0$ but close to it, Eq. 7 yields a frequency difference of the order of 30 kHz. This situation is illustrated in Fig. 12c.

5. CONCLUSIONS AND RECOMMENDATIONS

It has been established that plasma striation oscillations and multimodes contribute significantly to the noise level of gas lasers. For a HeNe laser operating at 6328Å striation oscillations may contribute as much as 20 db of noise over the shot noise within a range of frequencies extending from a few kHz to 100 kHz. Multimode operation may add another 20 db of noise if the modes are unlocked.

As a result of this investigation, the following steps are recommended for eliminating the excess noise:

a) Striation oscillation noise is reduced by increasing the available space charge over that normally adequate for the low current discharge; tube life is not adversely affected if a fairly large filament area is provided.

b) Multimode noise is minimized by eliminating off-axis modes through aperture reduction and particularly by avoiding near degenerate semiconfocal geometry.

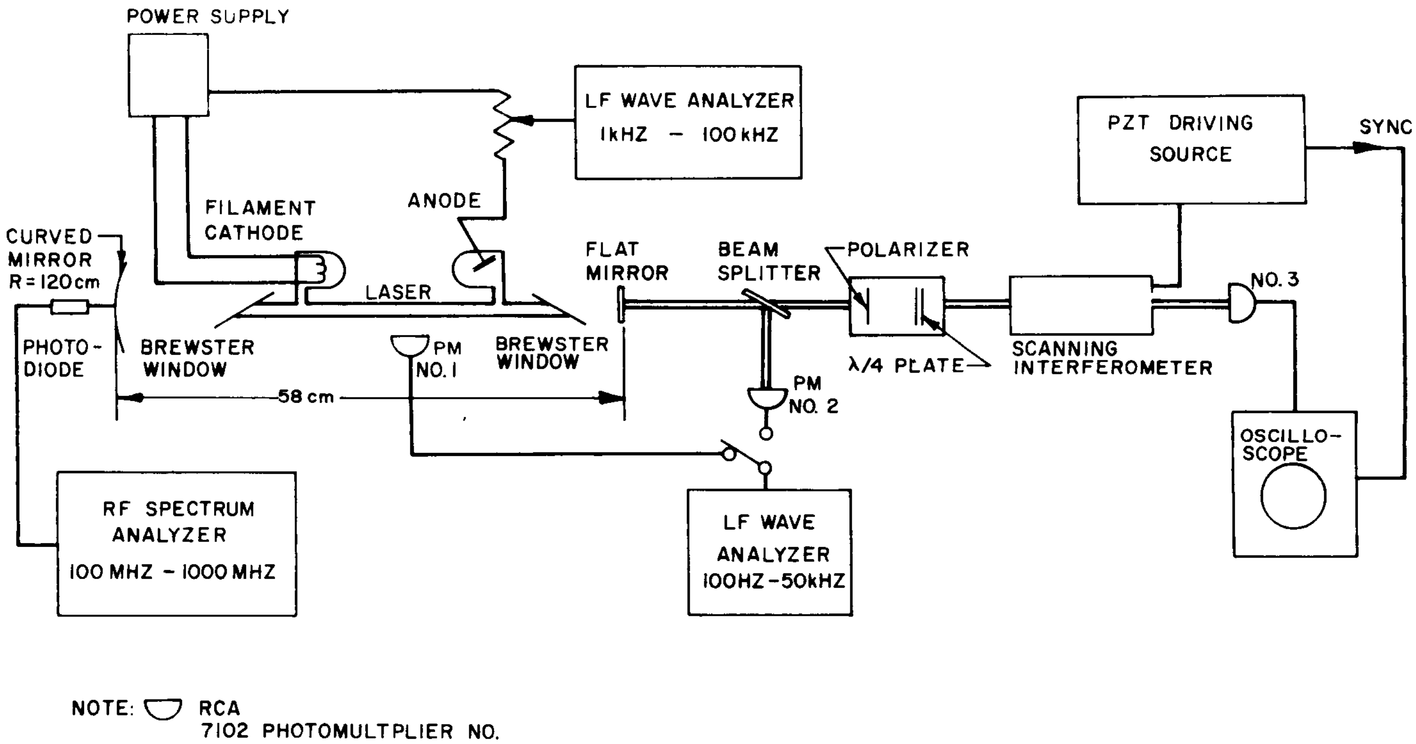

Figure 1a
Experiment setup

PA-3-10158

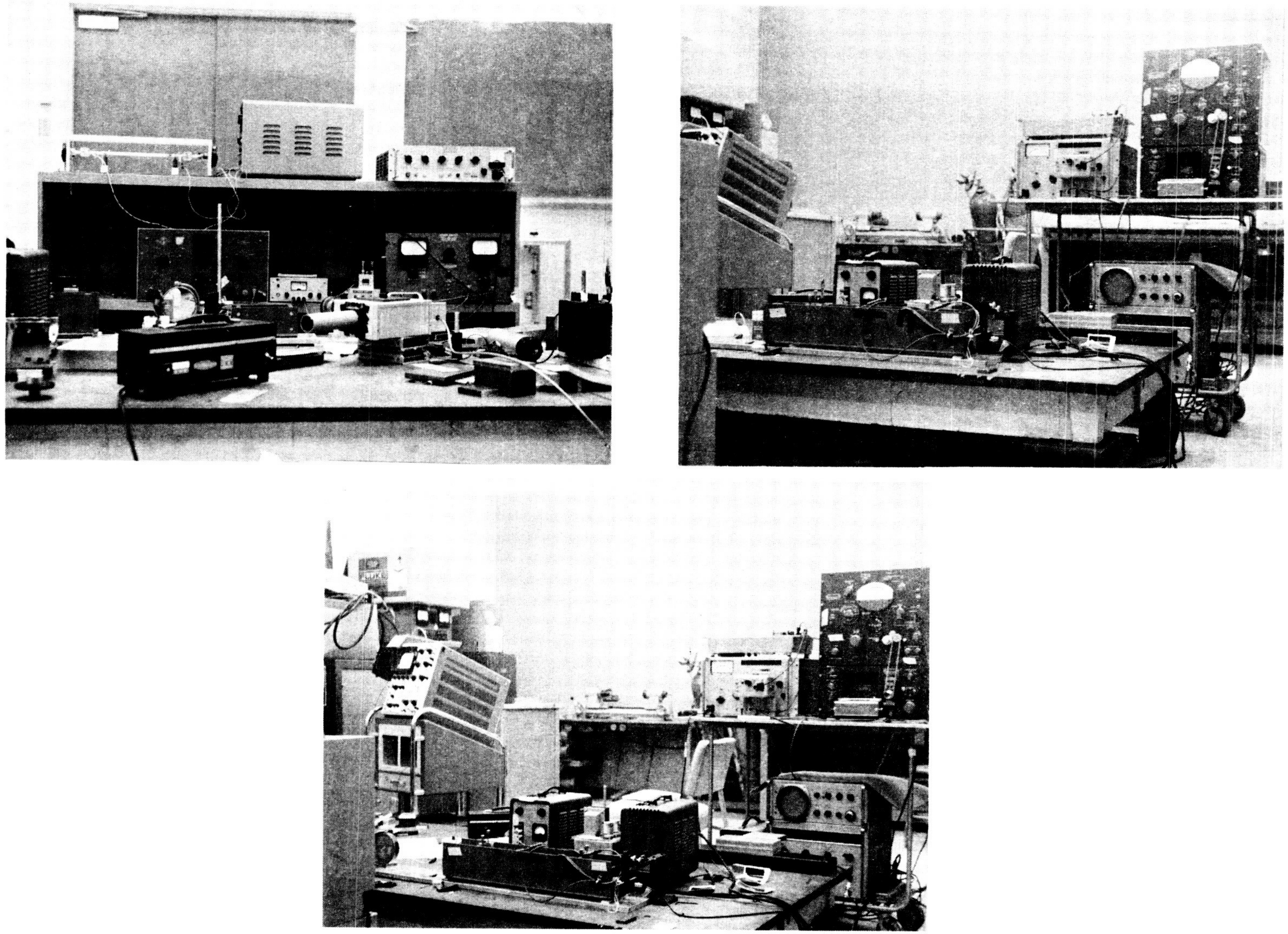

Figure 1b
Laboratory setup

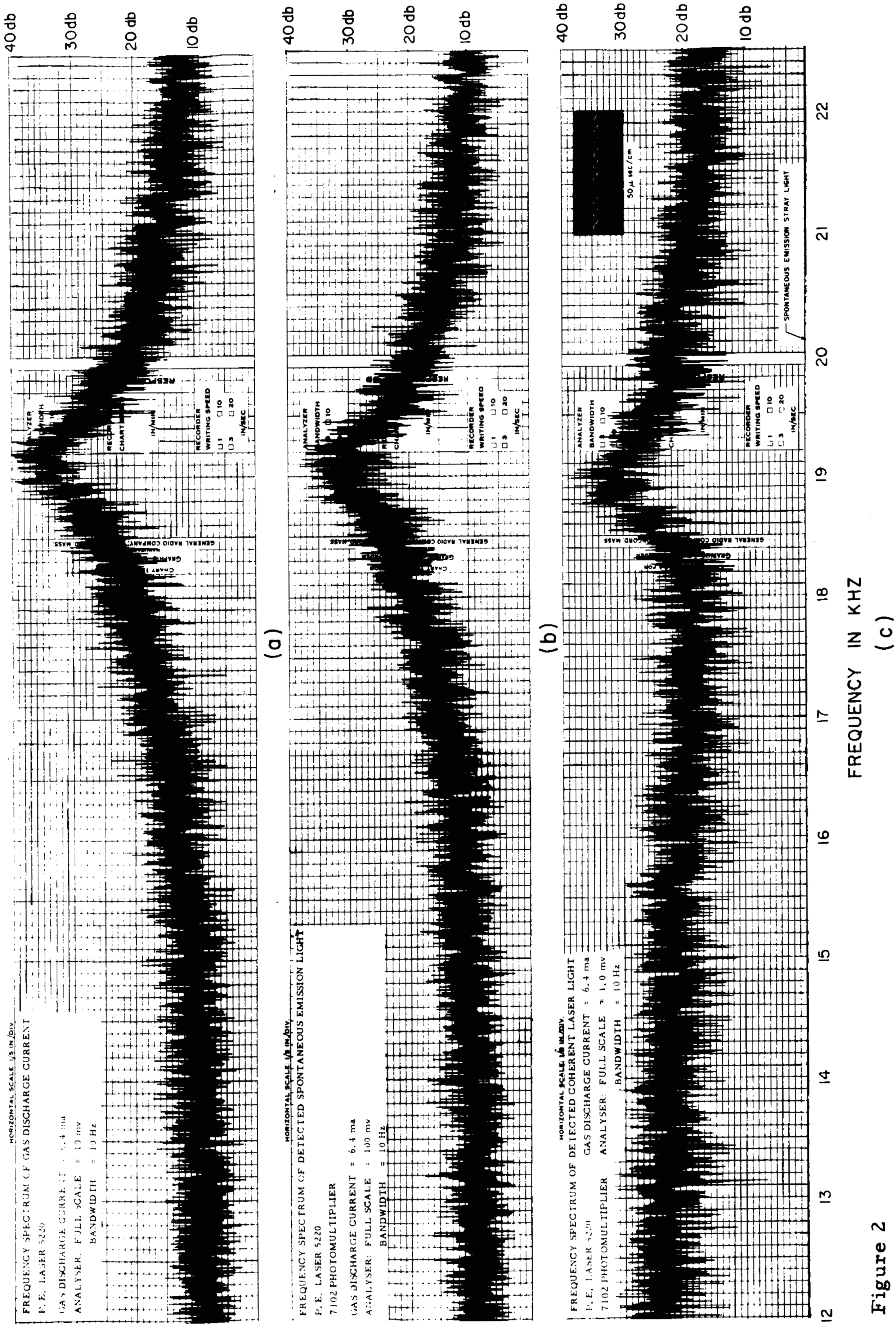

Figure 2
Fluctuations spectra

PA-3-10159

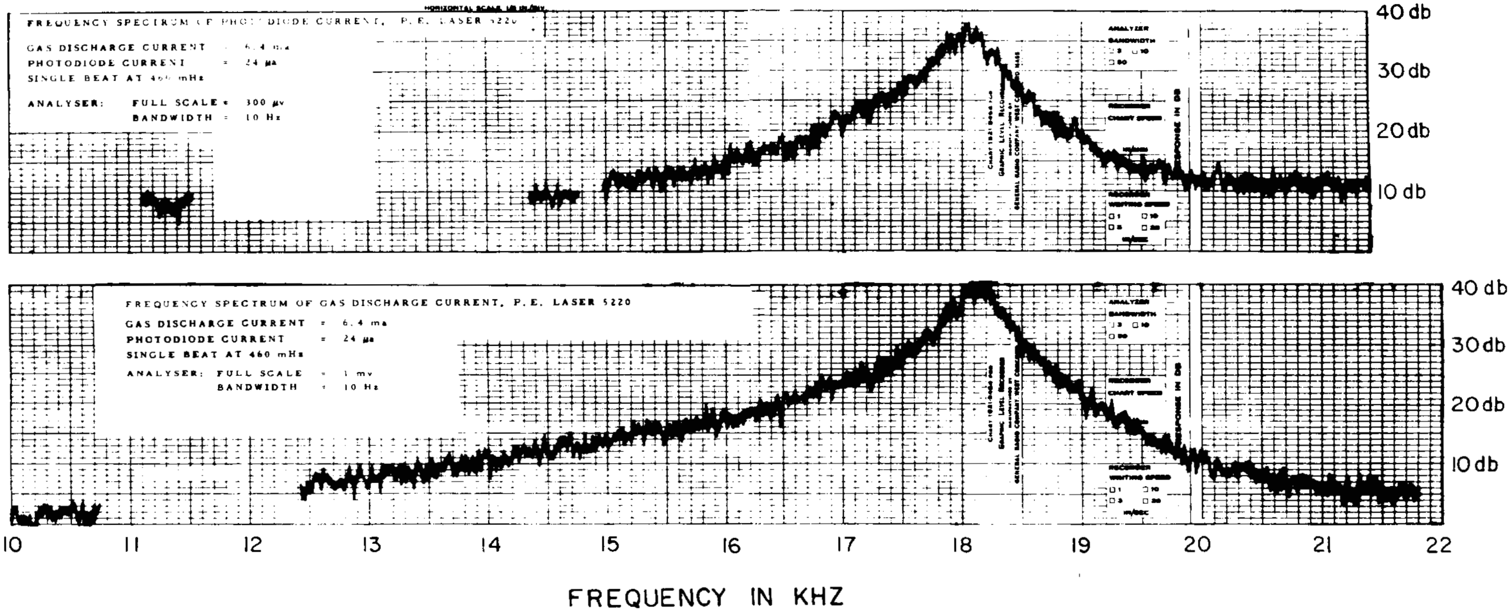

Figure 3
Fluctuations spectra

PA-3-10160

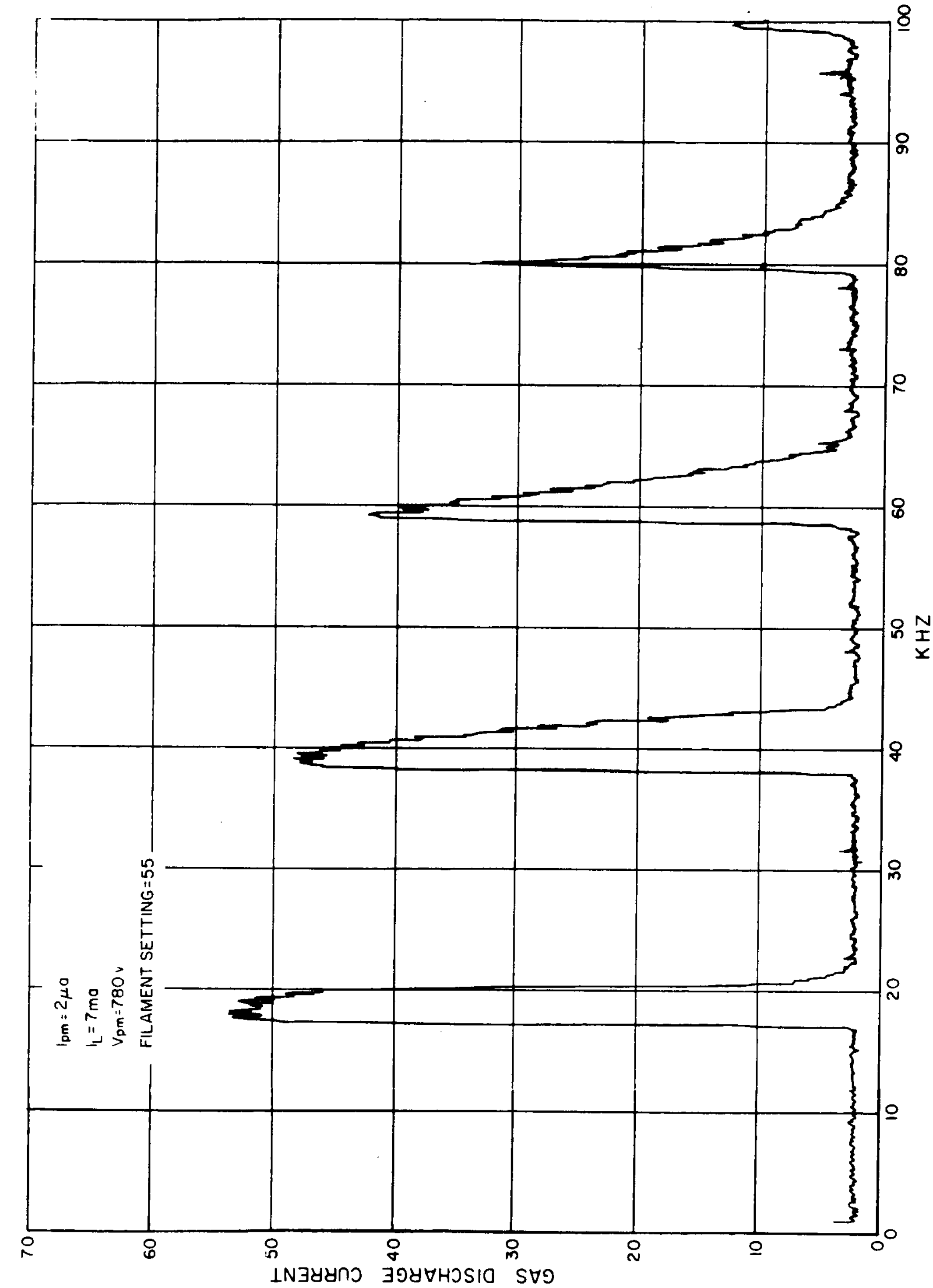

Figure 4a
Gas discharge current spectrum

PA-3-10161

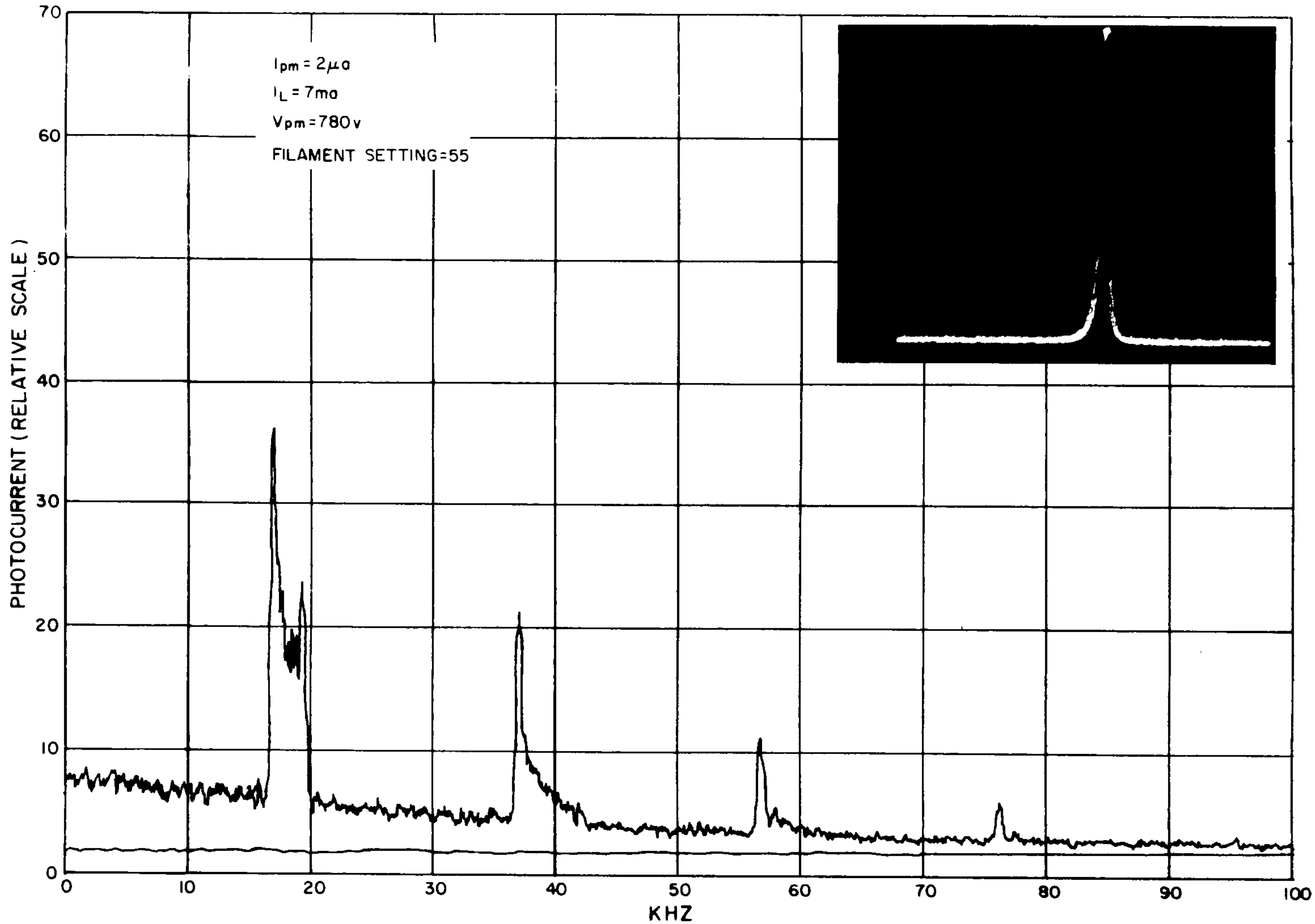

Figure 4b
Photocurrent spectrum (locked modes)

PA-3-10162

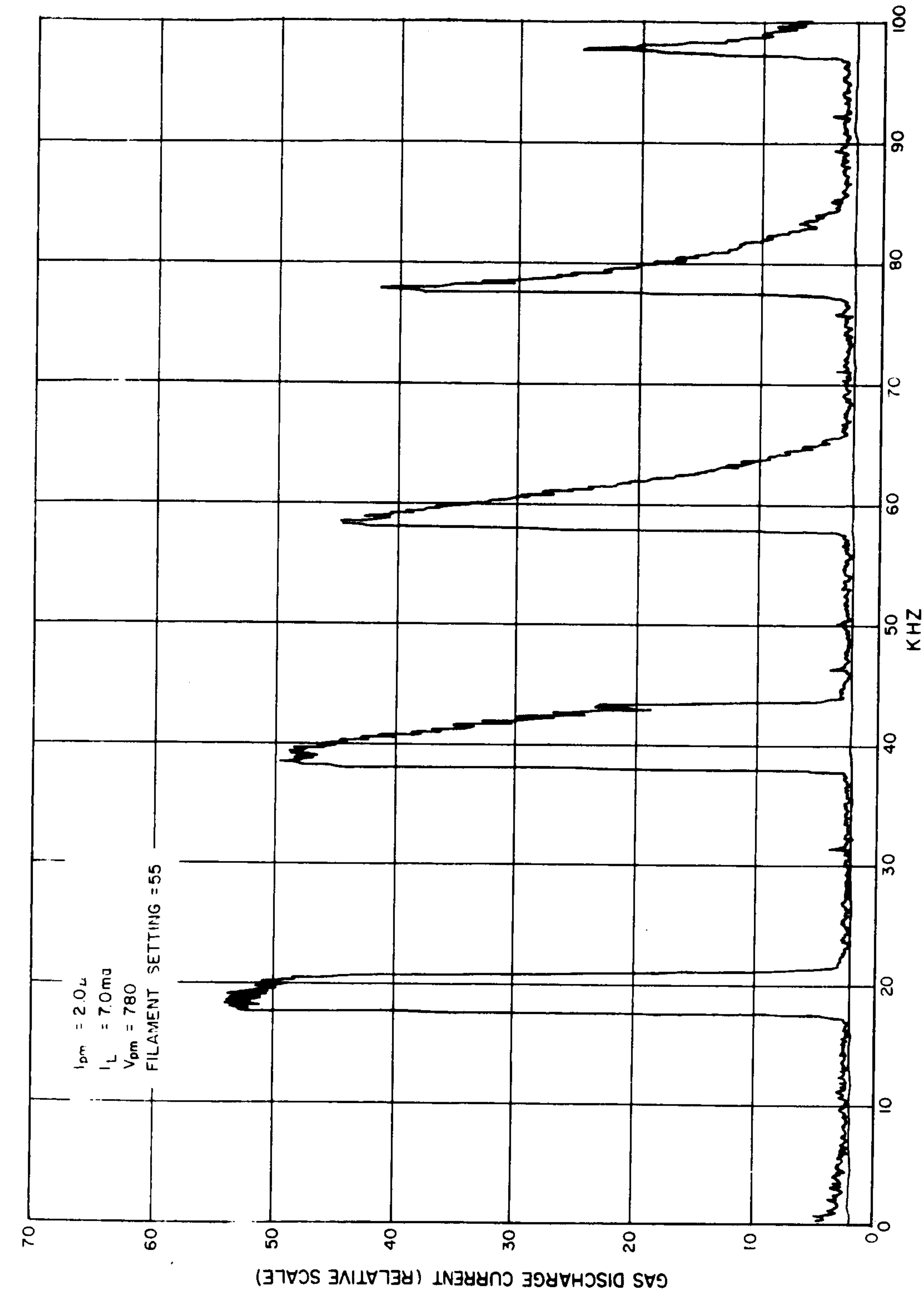

Figure 5a
Gas discharge current spectrum

PA-3-10163

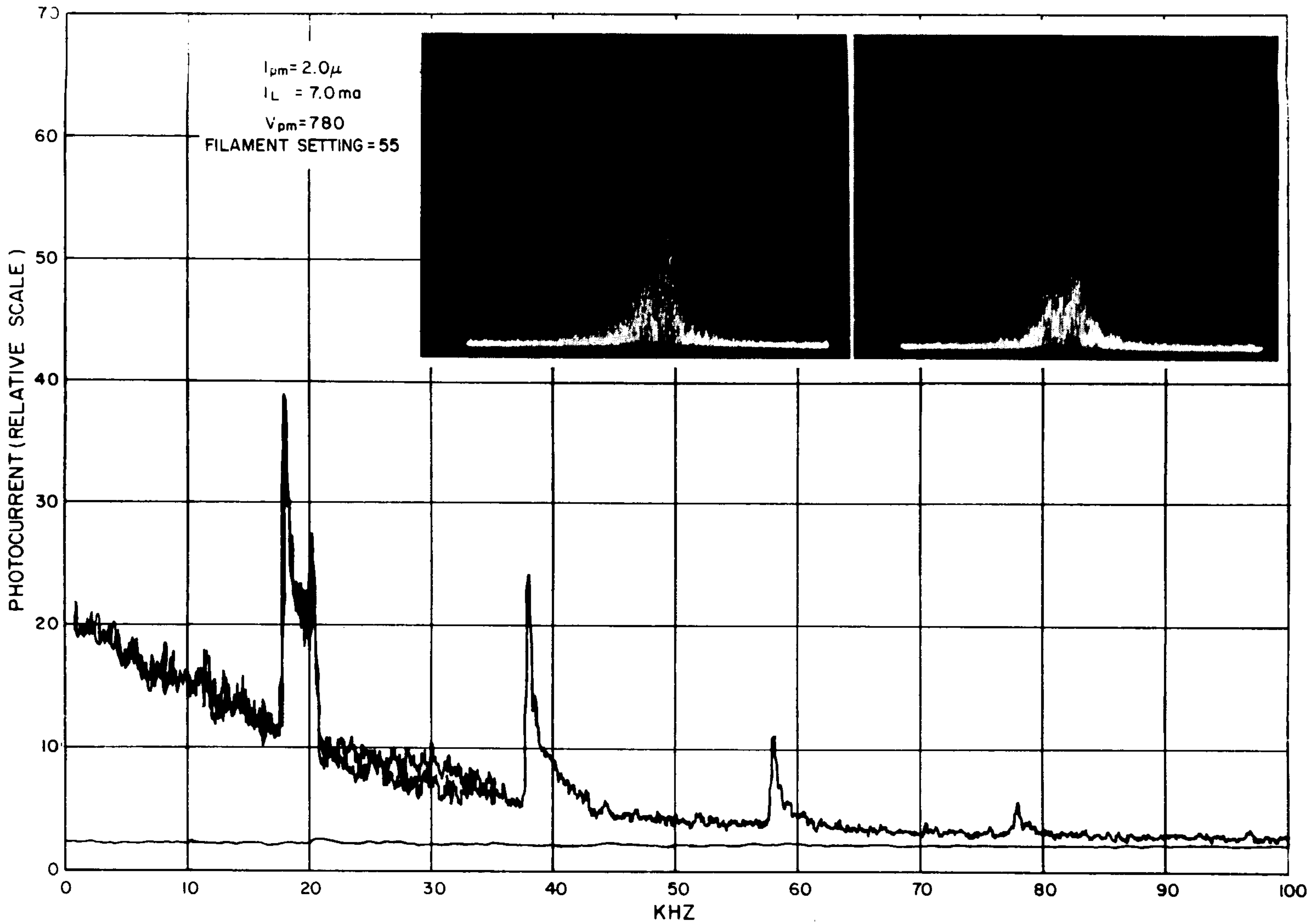

Figure 5b

Photocurrent spectrum (unlocked modes)

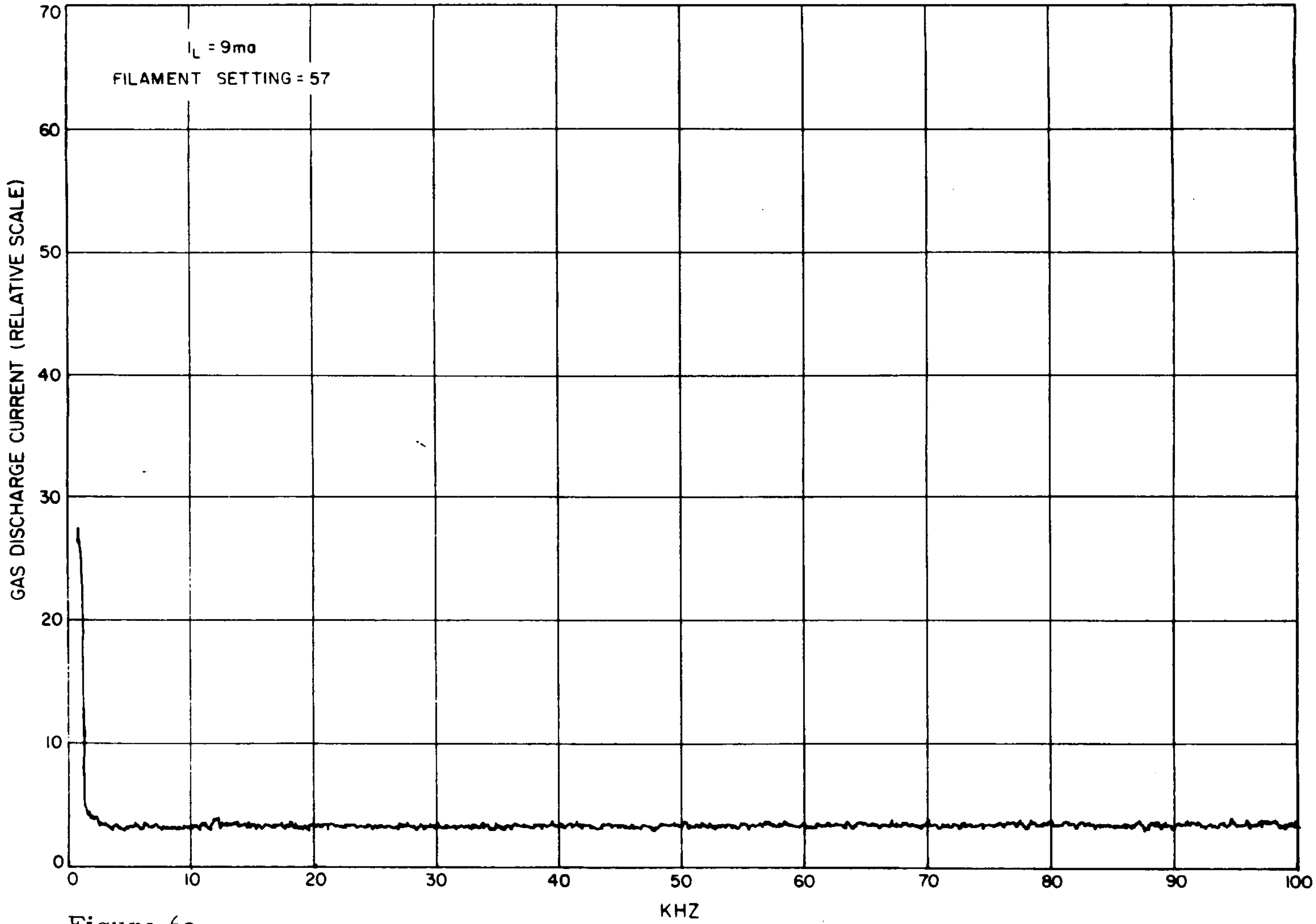

Figure 6a

Gas discharge current spectrum

PA-3-10165

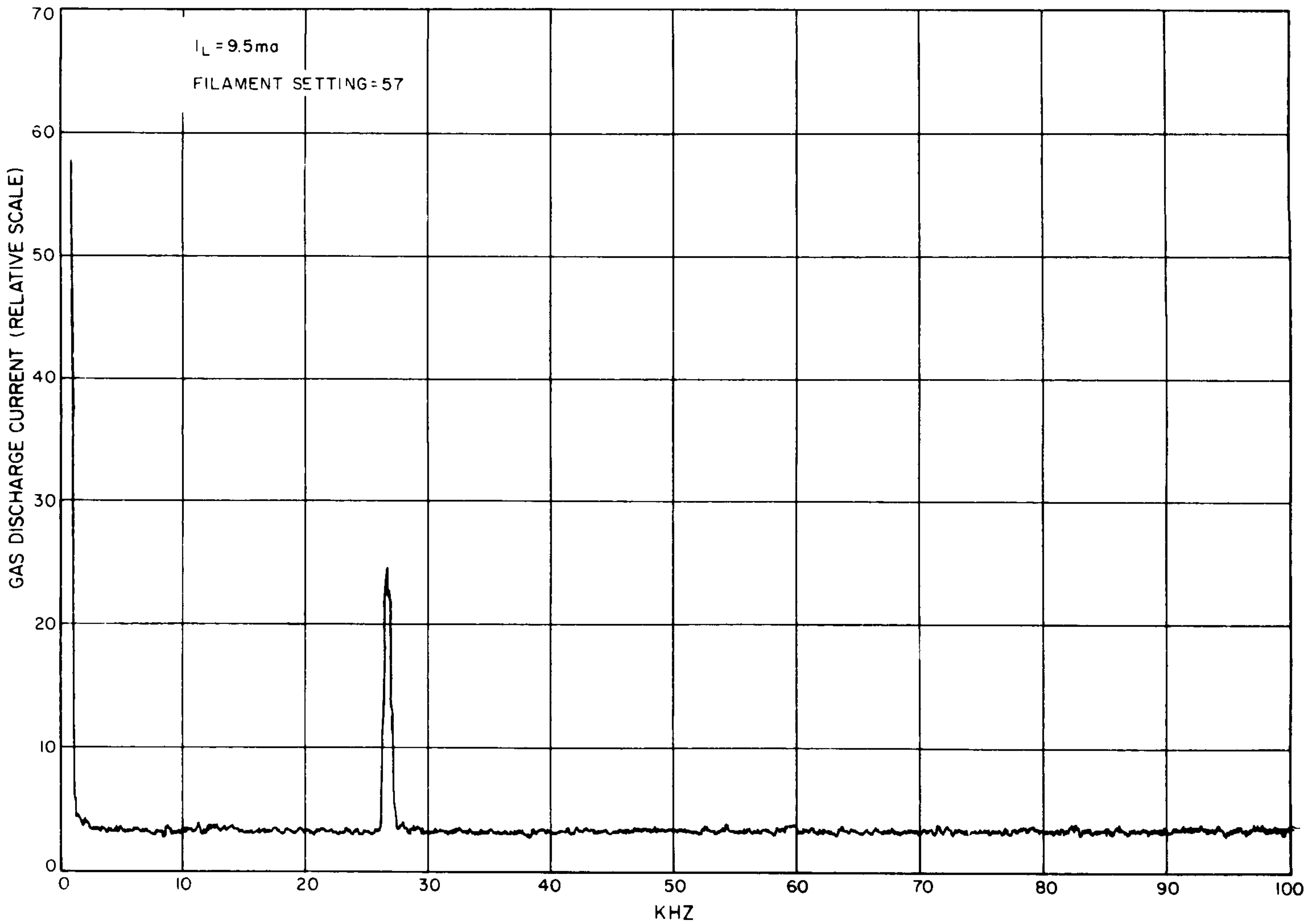

Figure 6b

Gas discharge current spectrum

PA-3-10166

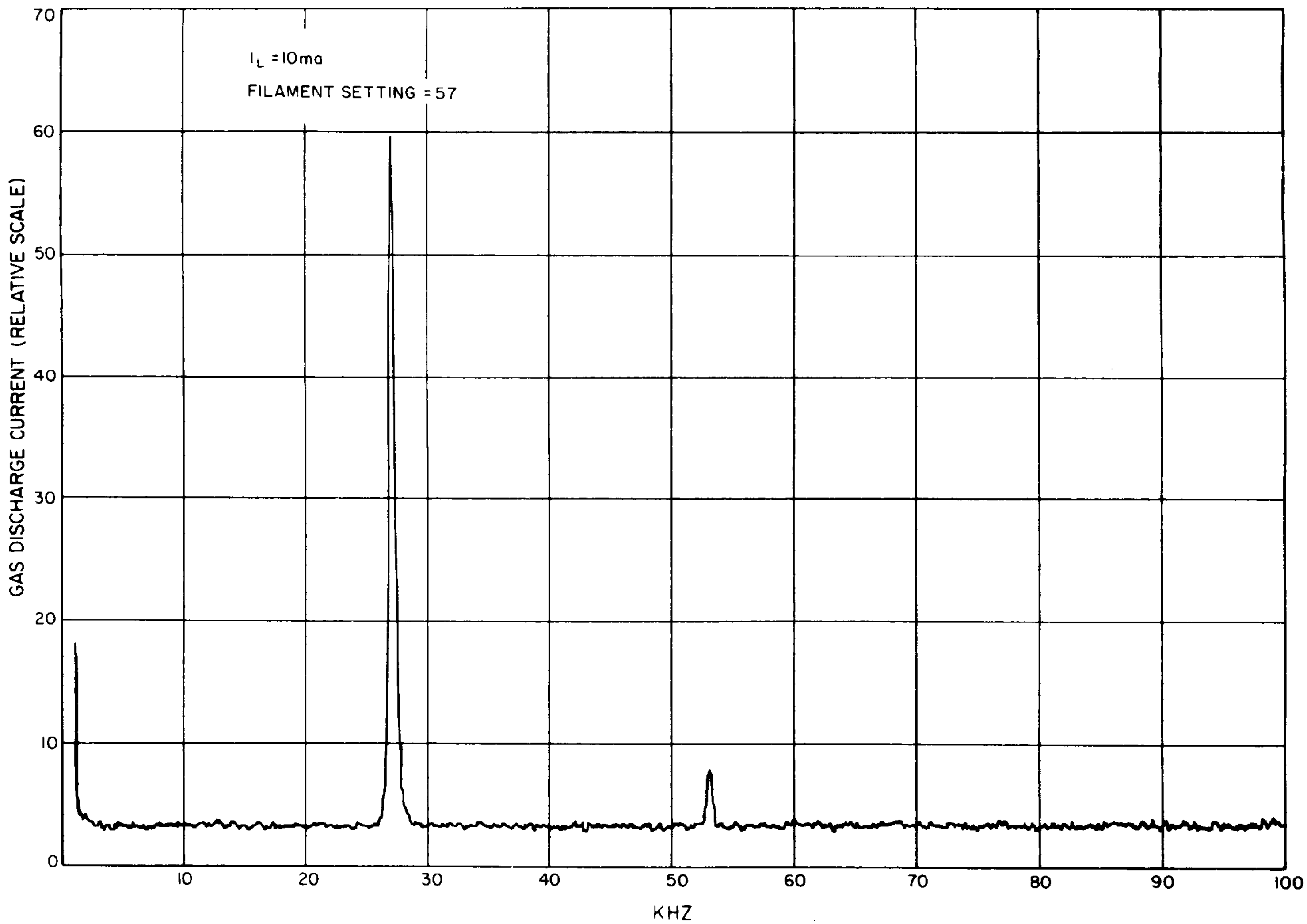

Figure 6c
Gas discharge current spectrum

PA-3-10167

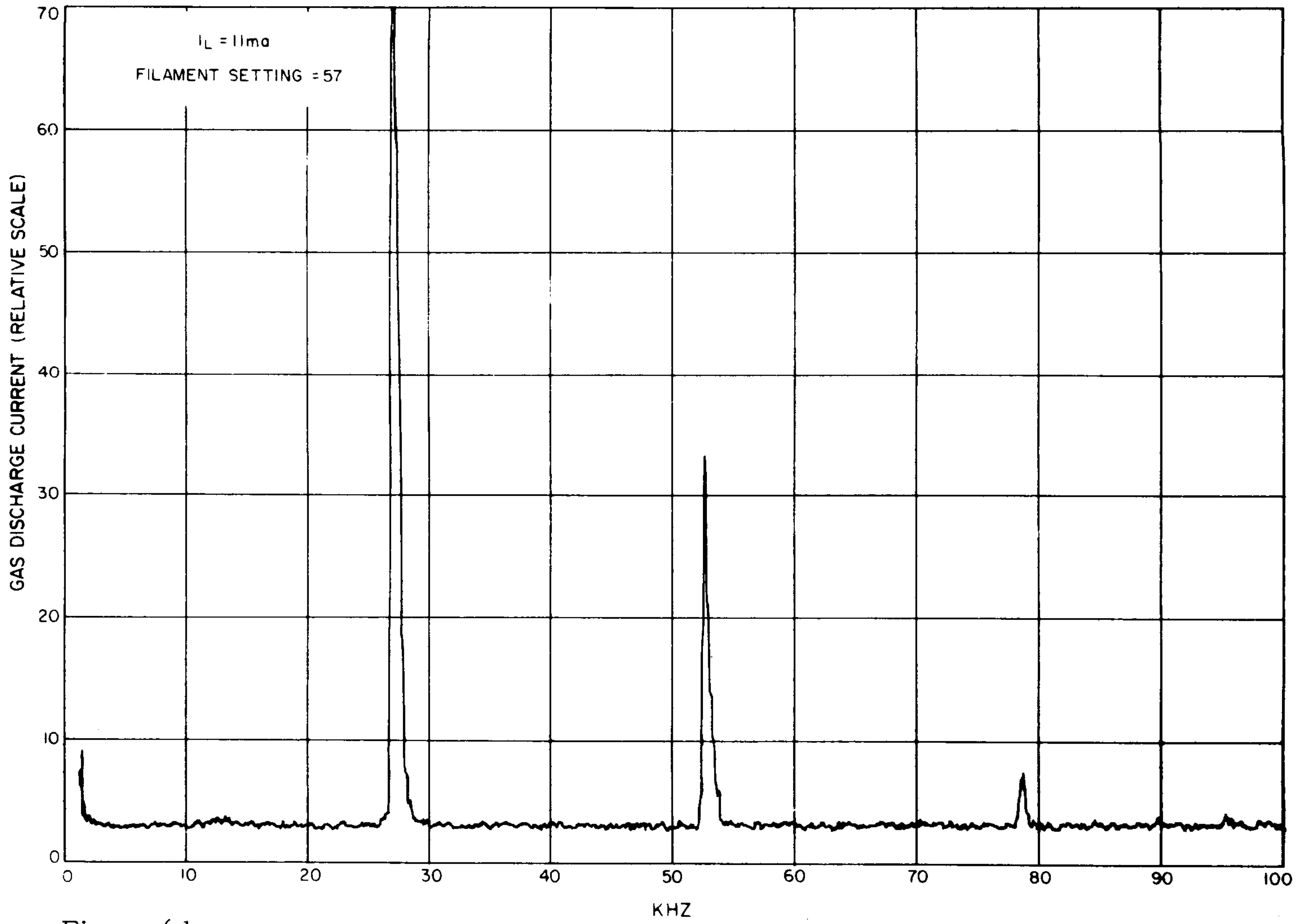

Figure 6d
Gas discharge current spectrum

PA-3-10168

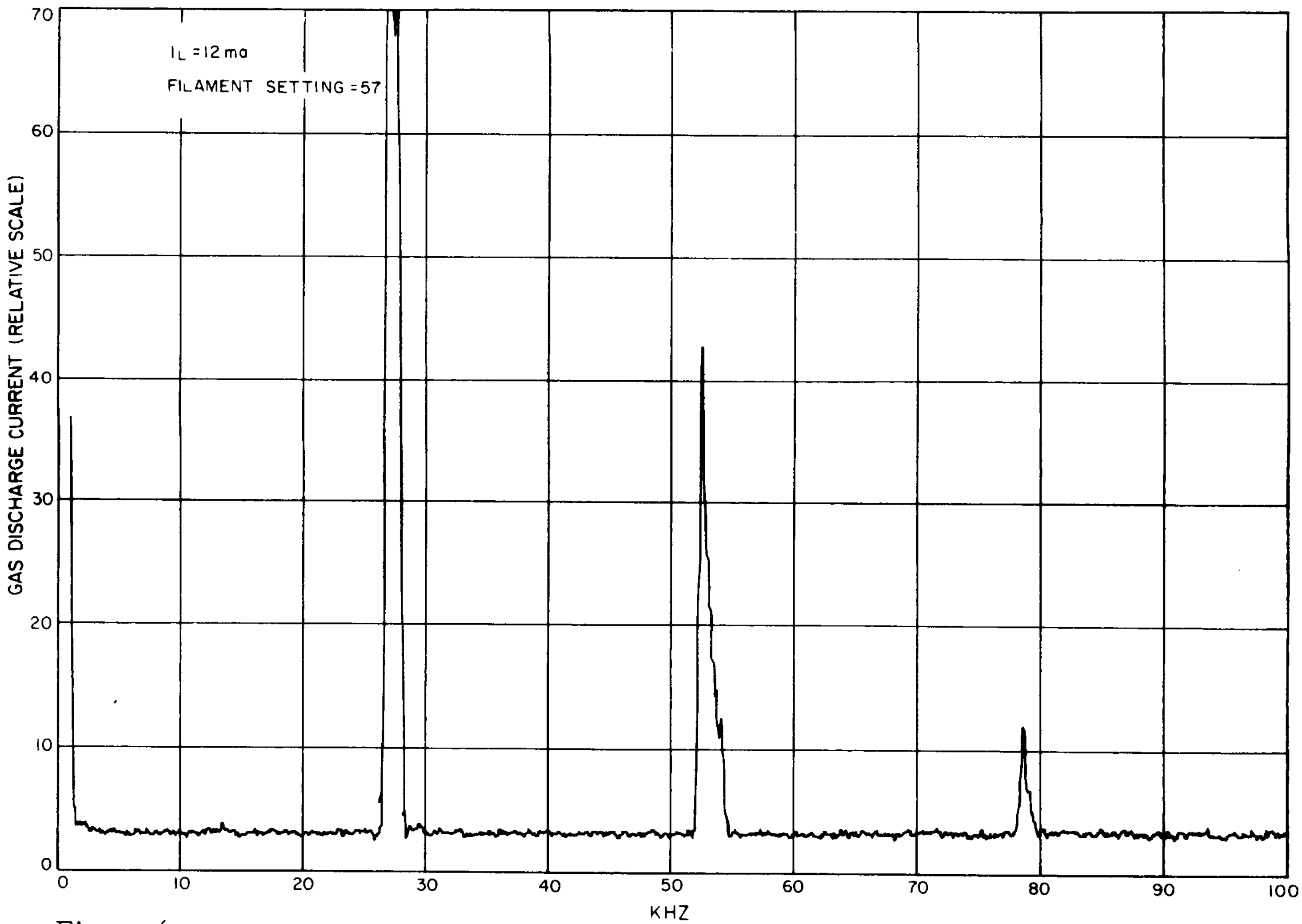

Figure 6e
Gas discharge current spectrum

PA-3-10169

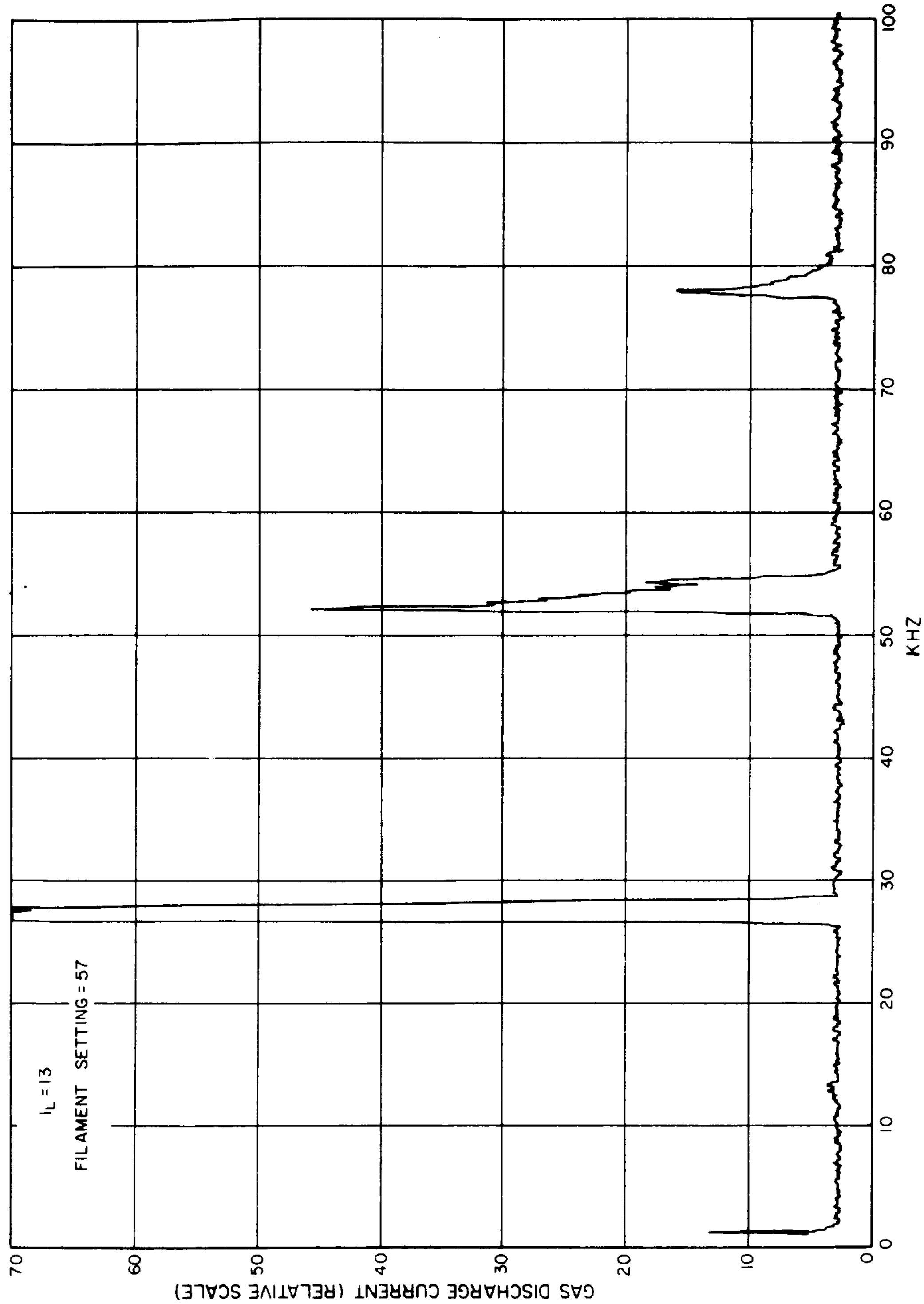

Figure 6f
Gas discharge current spectrum

PA-3-10170

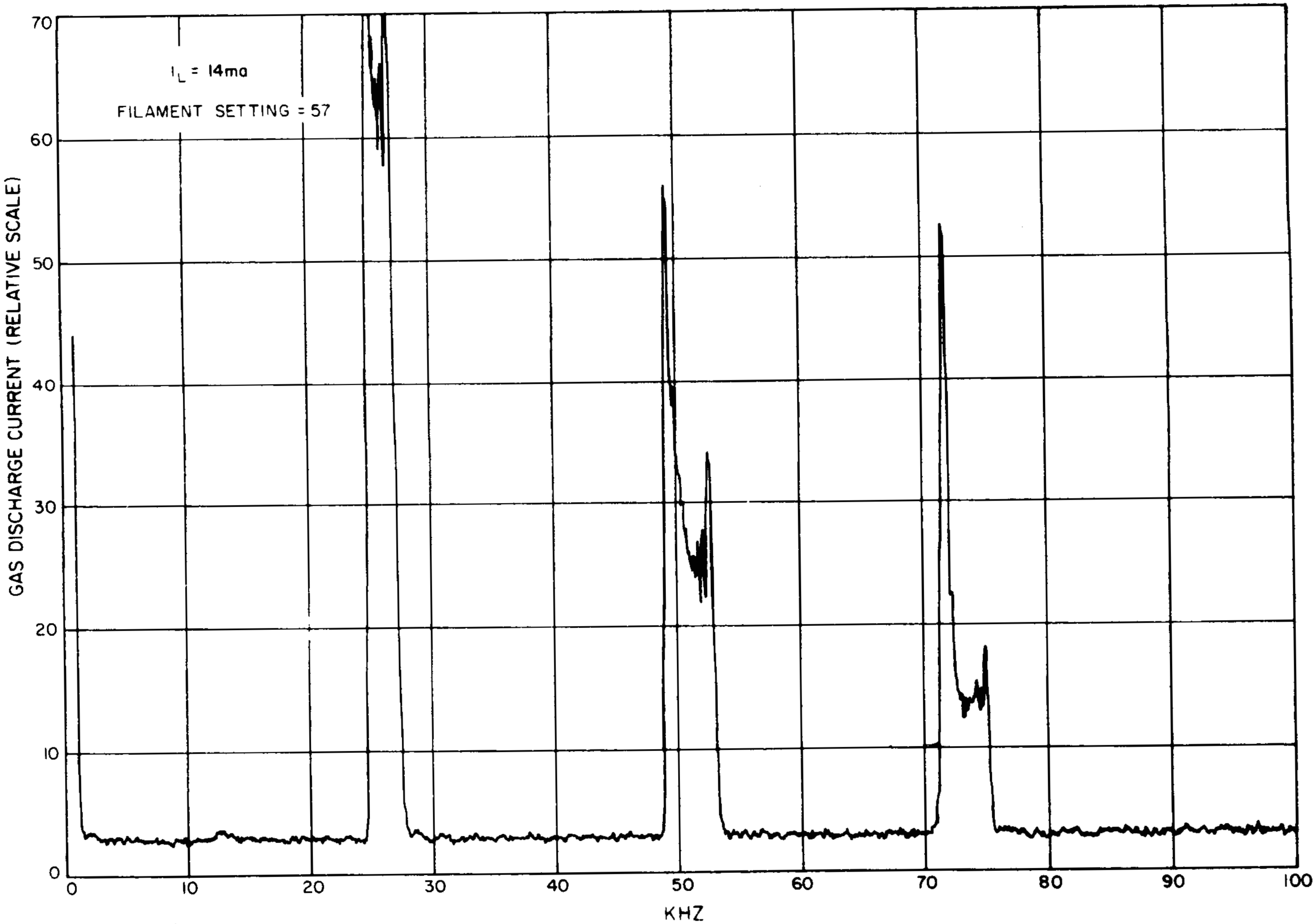

Figure 6g

Gas discharge current spectrum

PA-3-10171

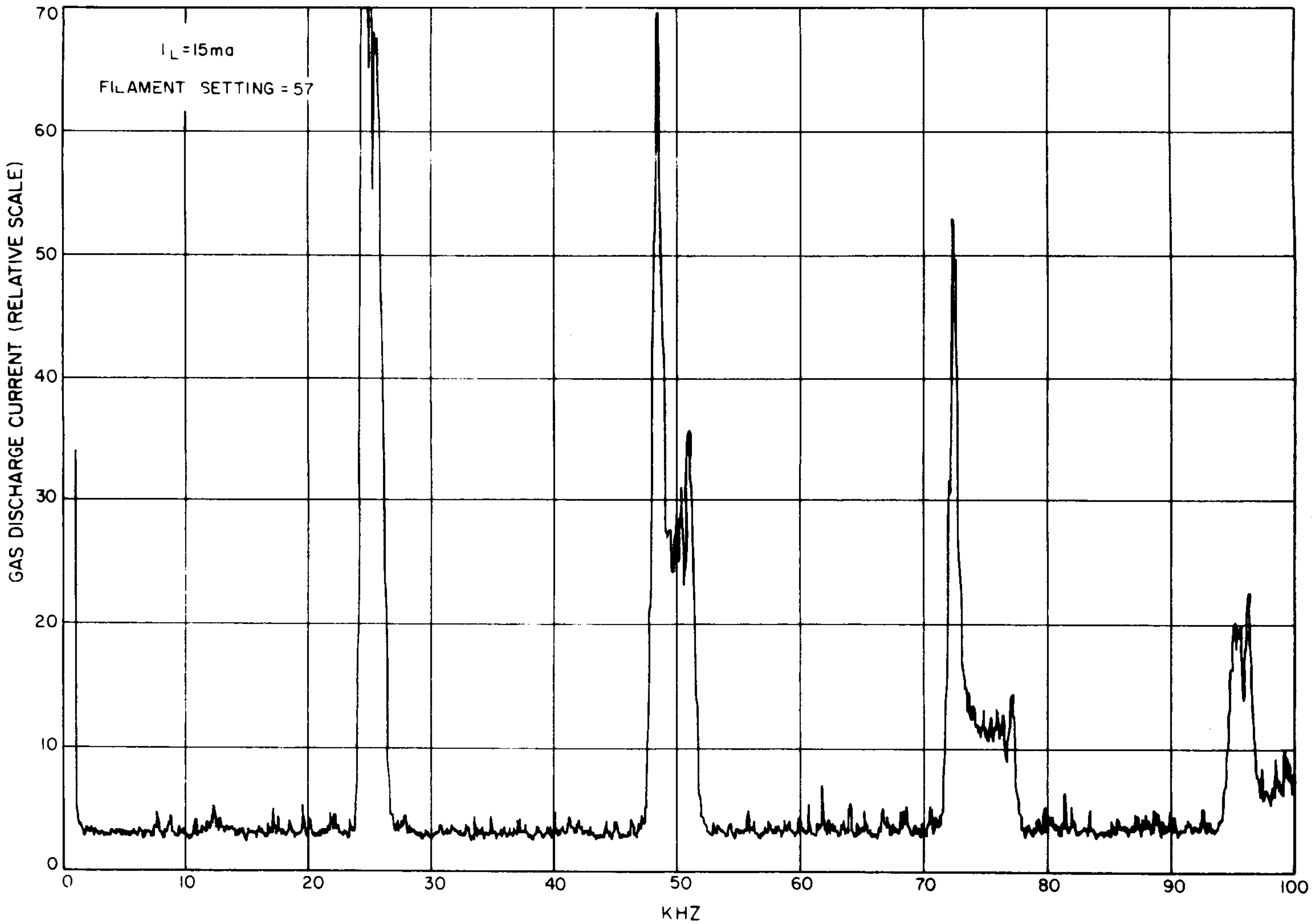

Figure 6h

Gas discharge current spectrum

PA-3-10172

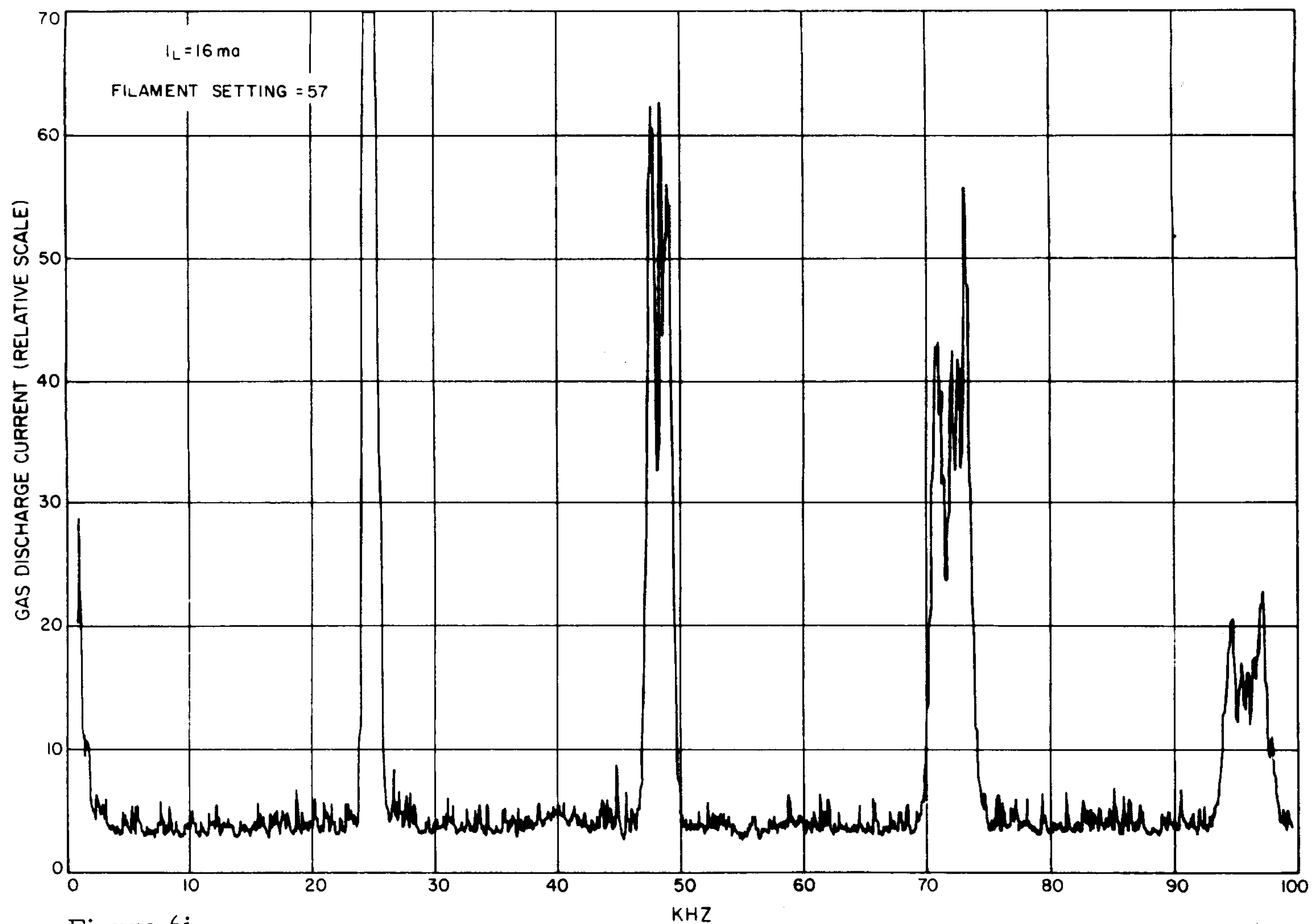

Figure 6i

Gas discharge current spectrum

PA-3-10173

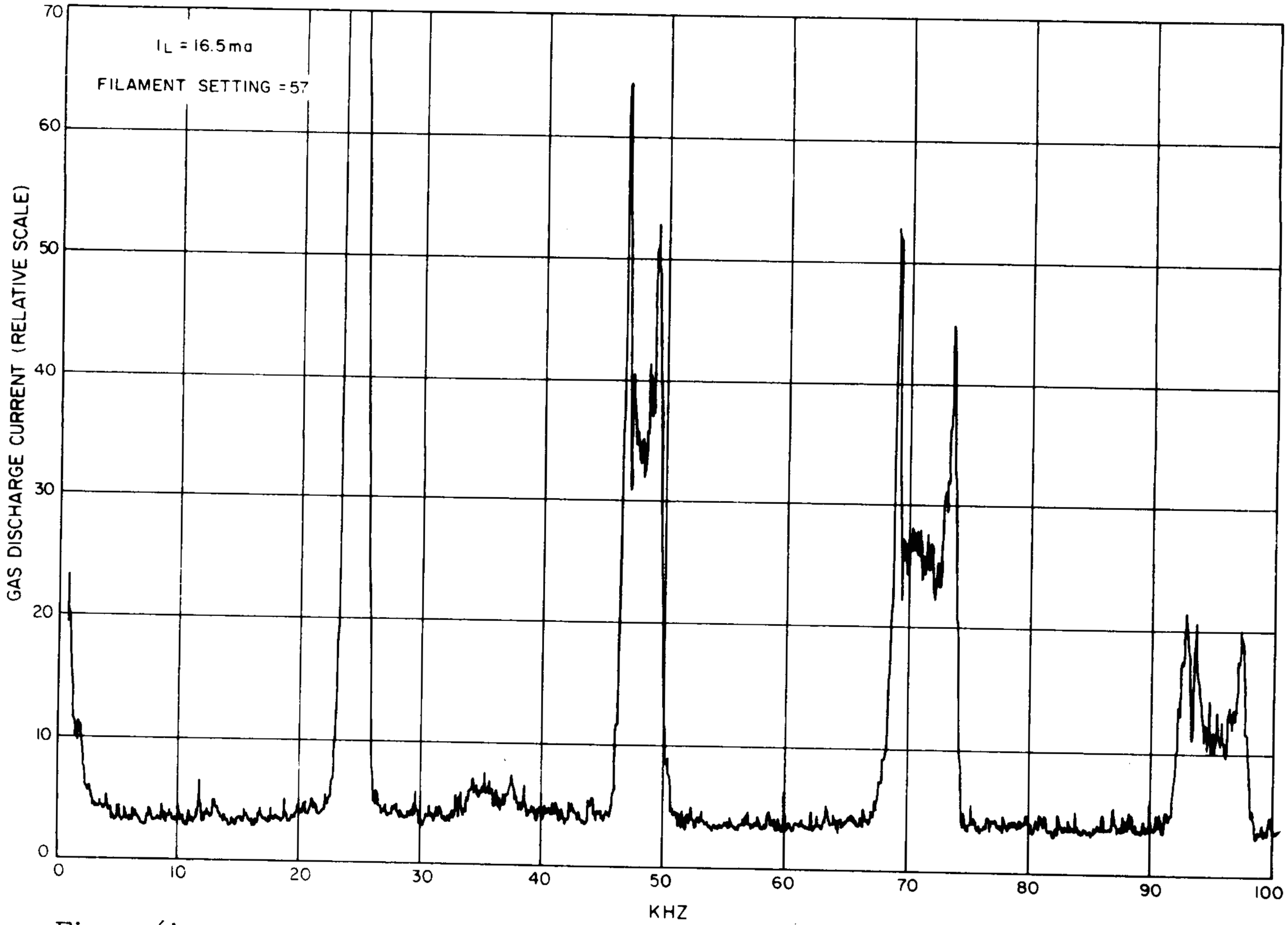

Figure 6j
Gas discharge current spectrum

PA-3-10174

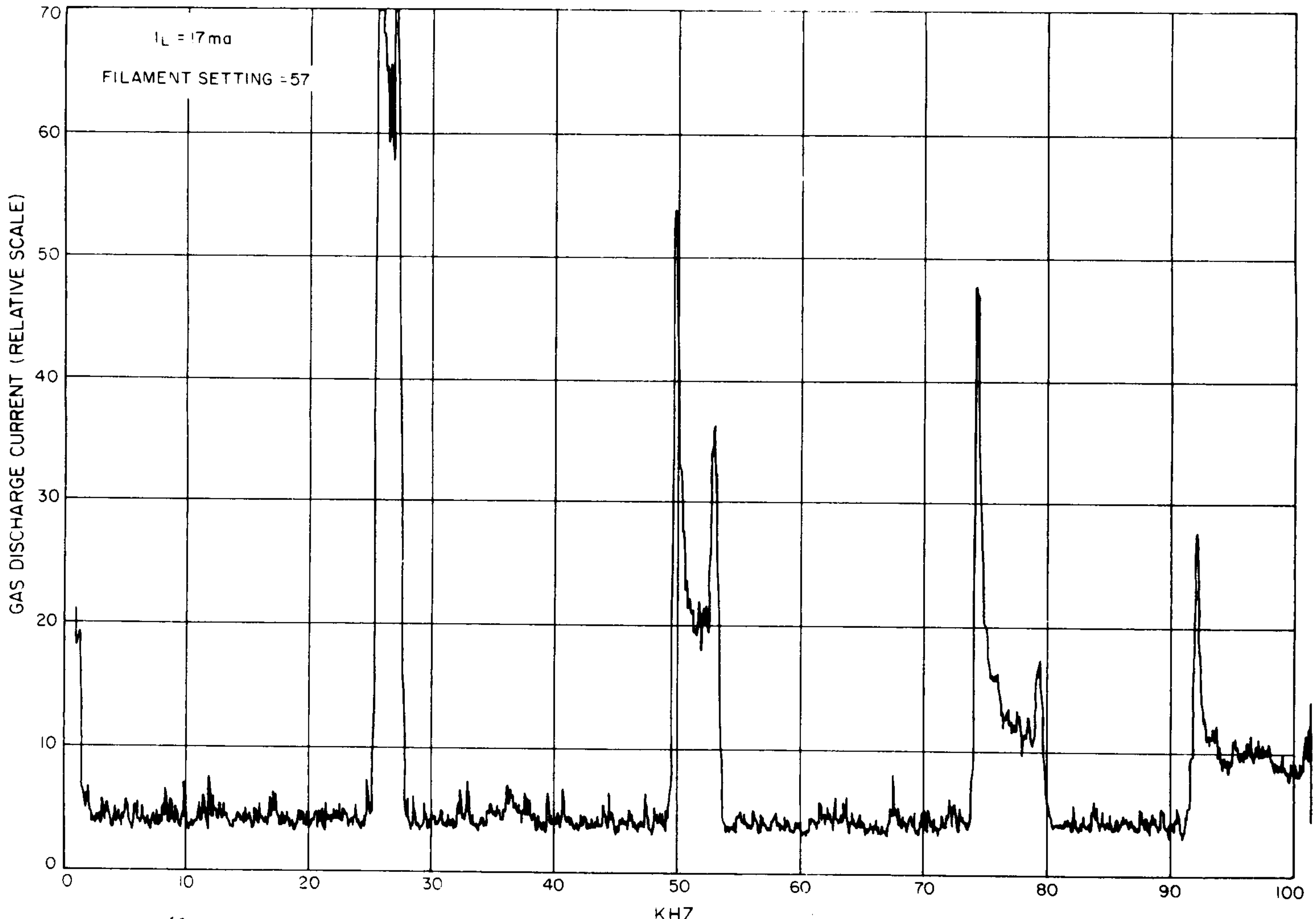

Figure 6k
Gas discharge current spectrum

PA-3-10175

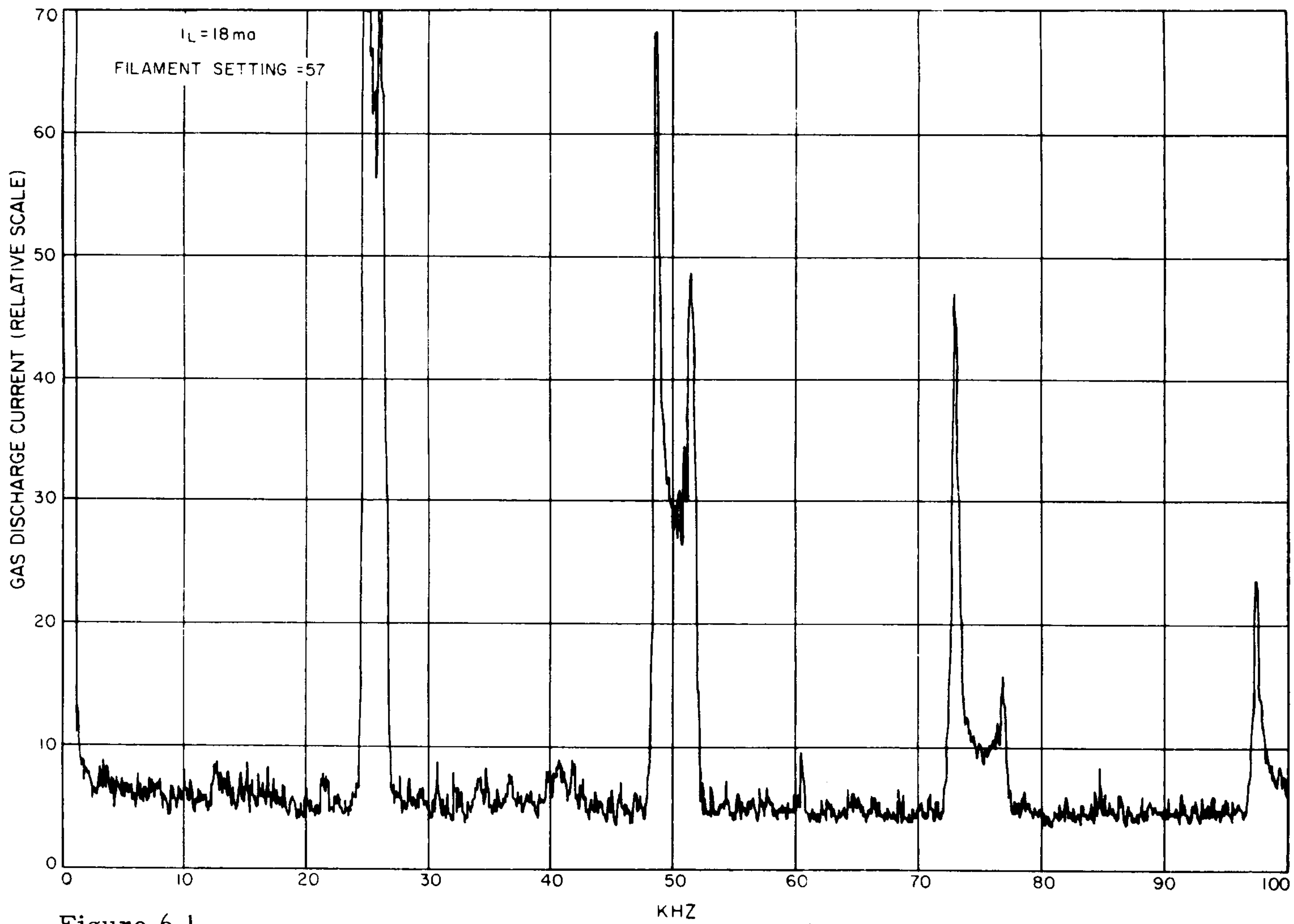

Figure 6 1

Gas discharge current spectrum

PA-3-10176

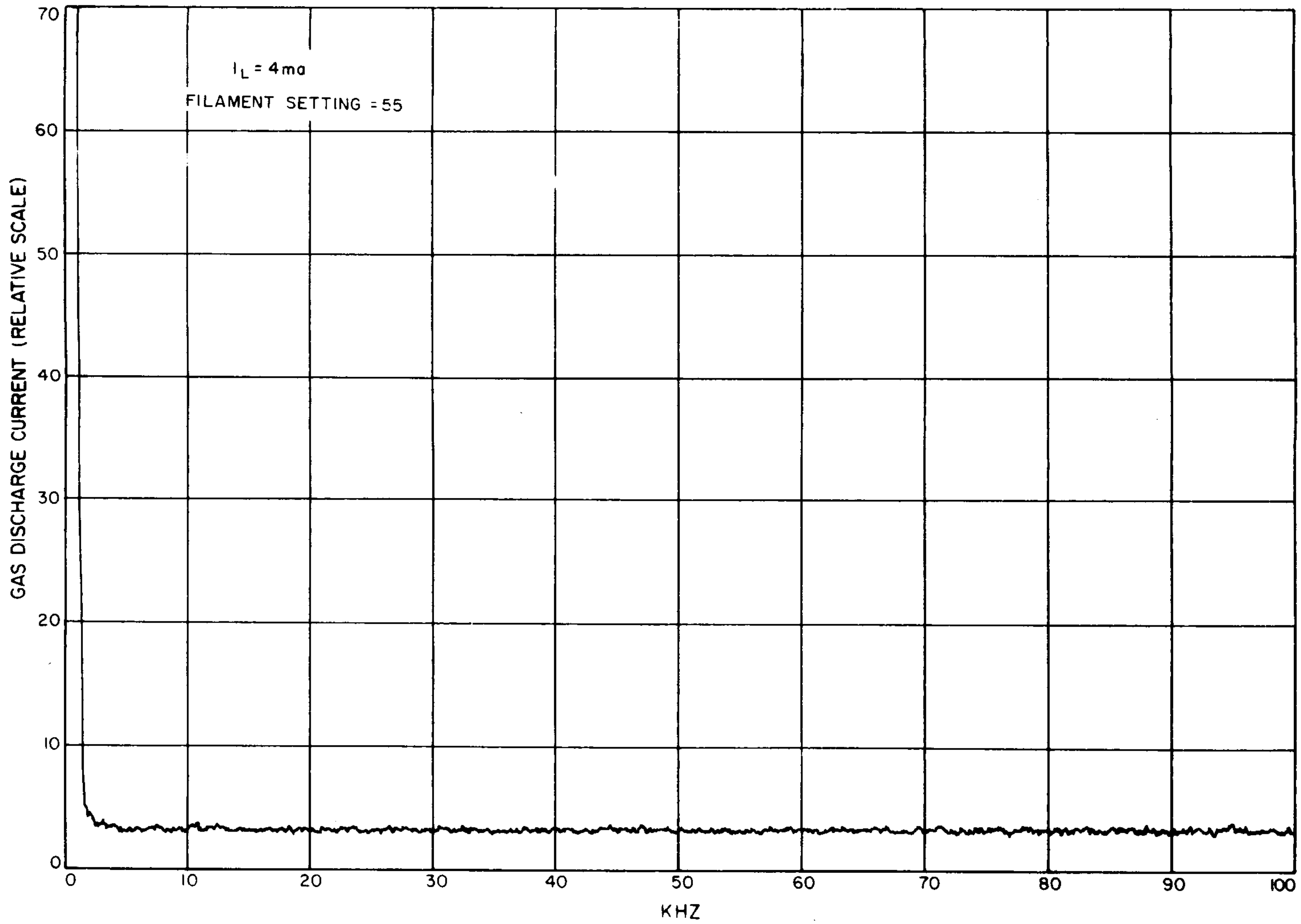

Figure 7a

Gas discharge current spectrum

PA-3-10177

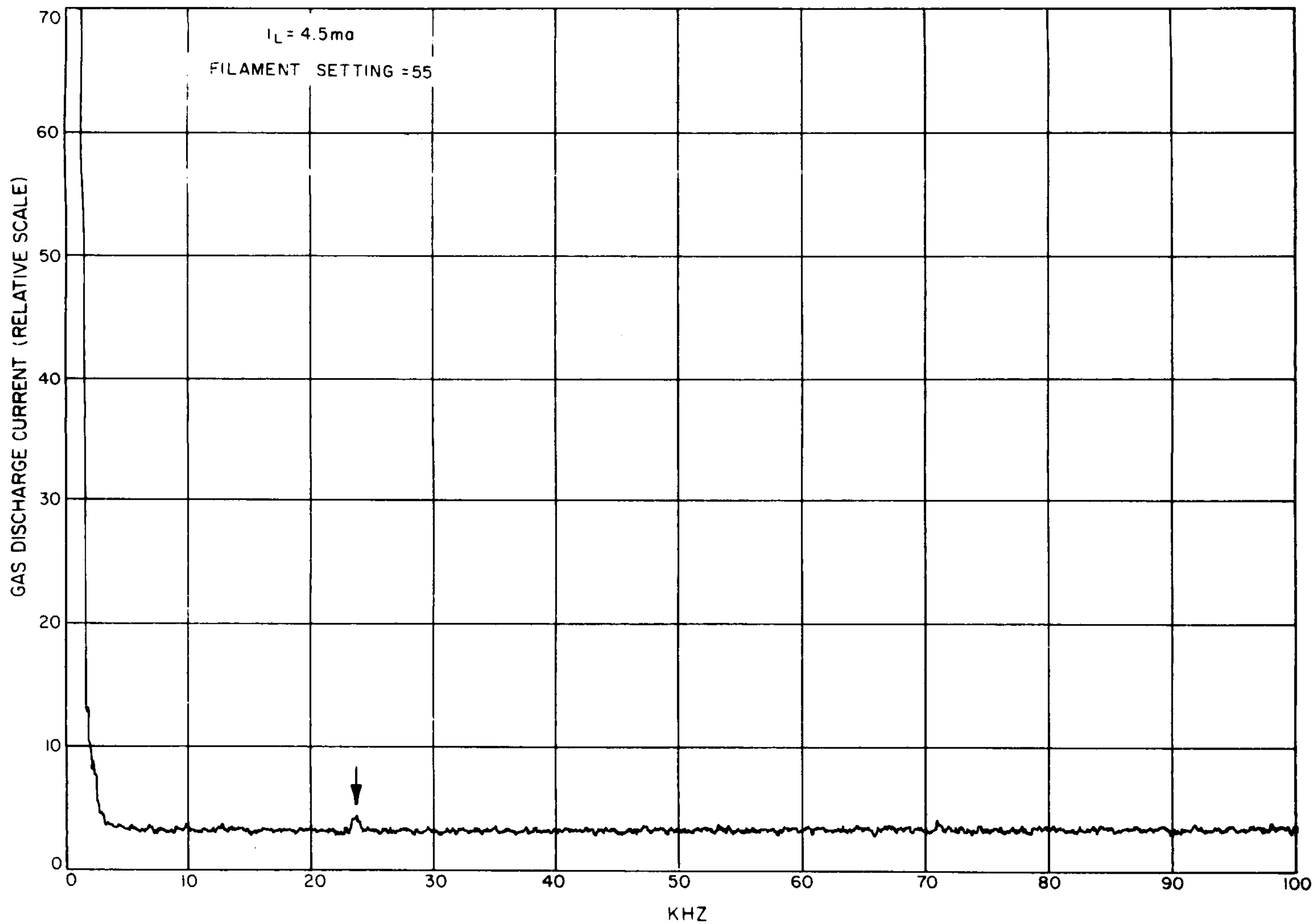

Figure 7b
Gas discharge current spectrum

PA-3-10178

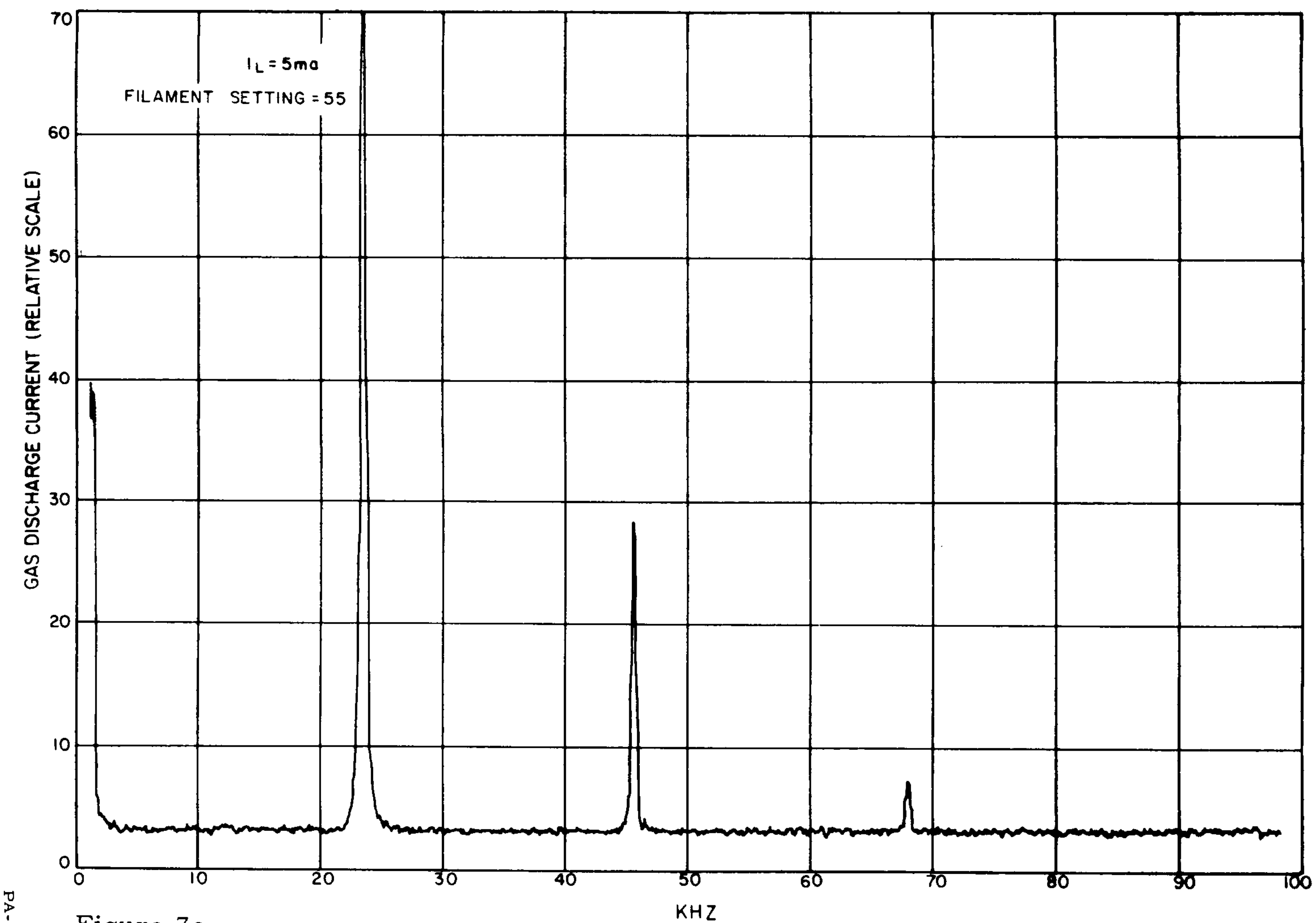

Figure 7c

Gas discharge current spectrum

PA-3-10179

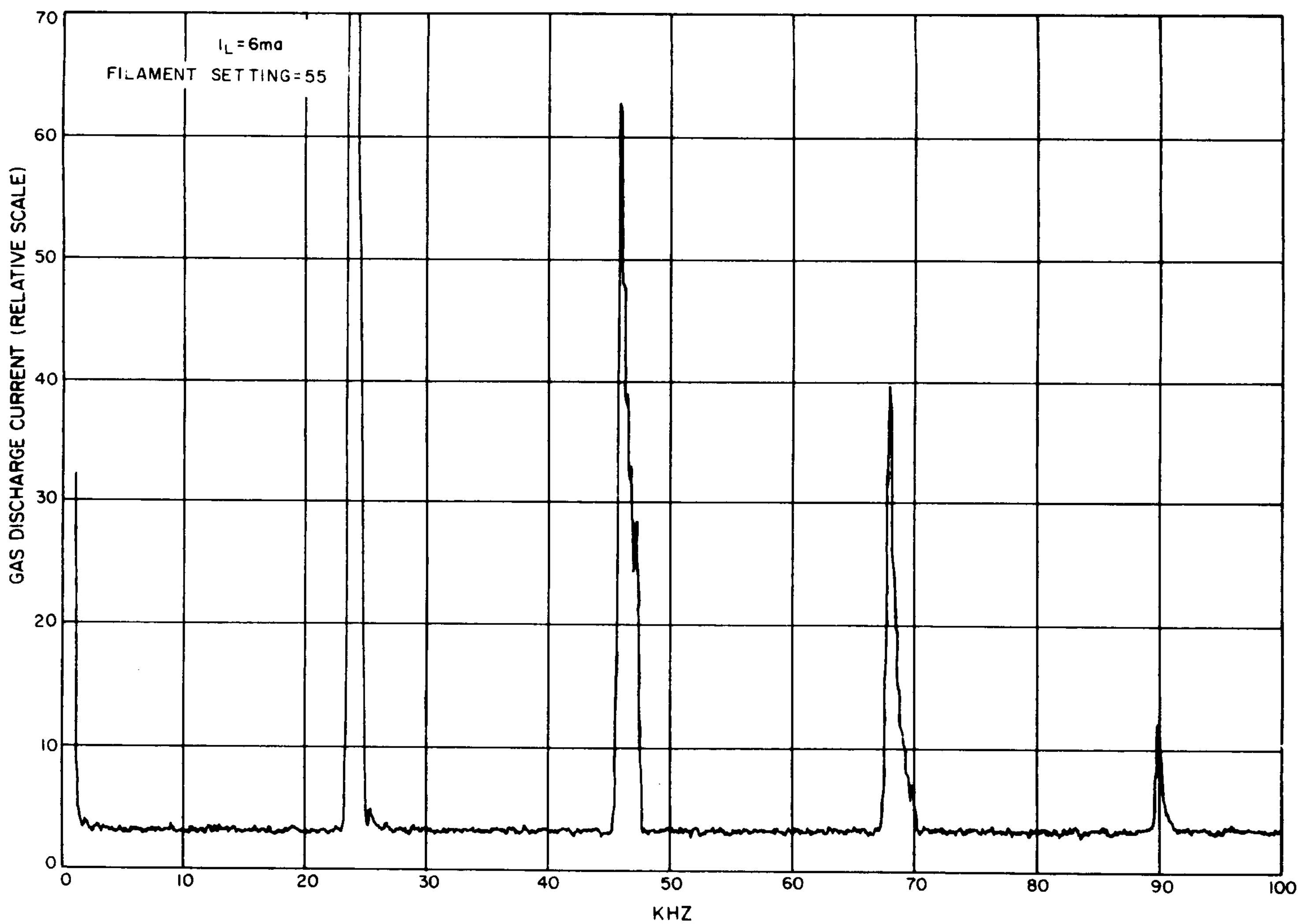

Figure 7d

Gas discharge current spectrum

PA-3-10180

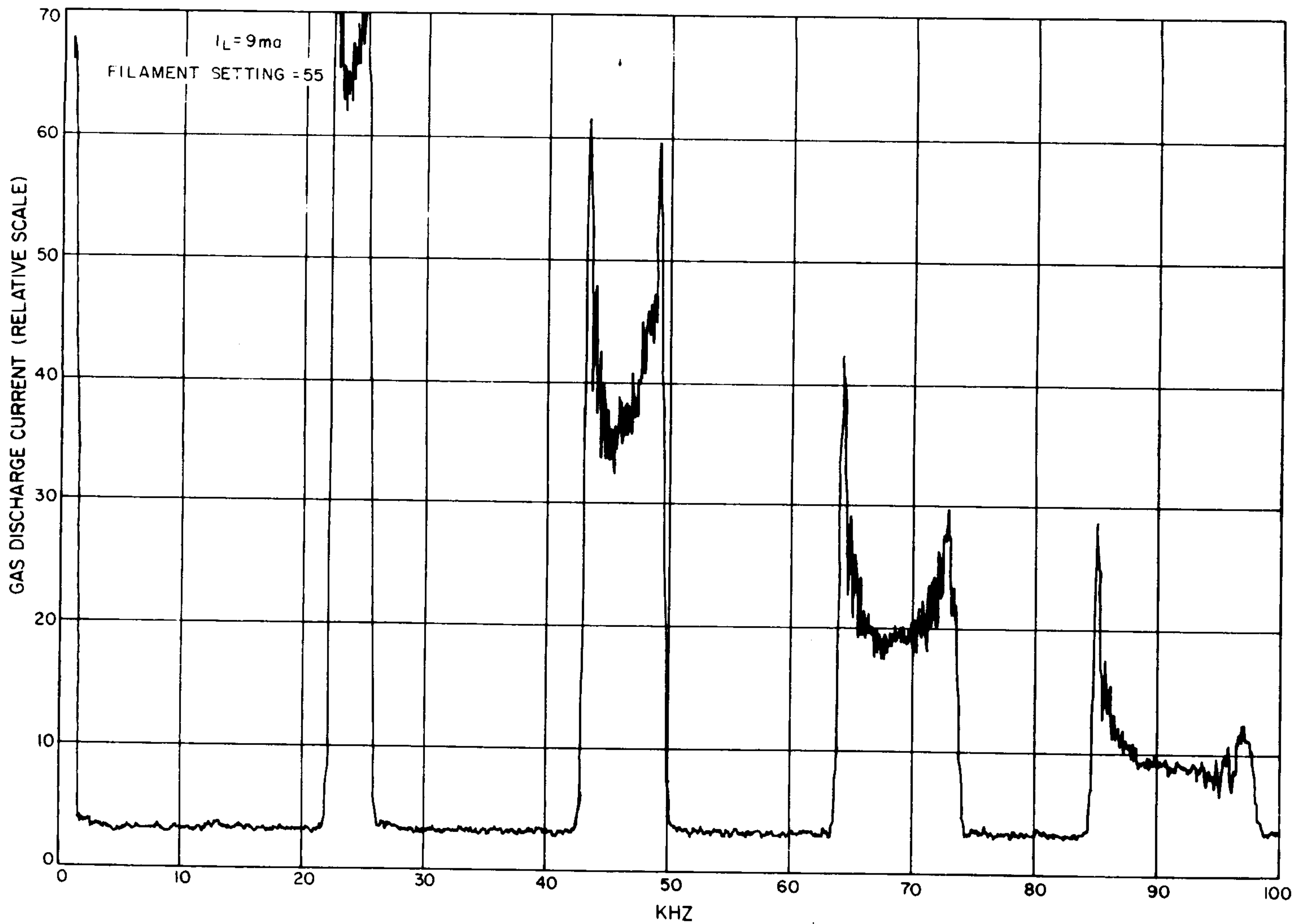

Figure 7e
Gas discharge current spectrum

PA-3-10181

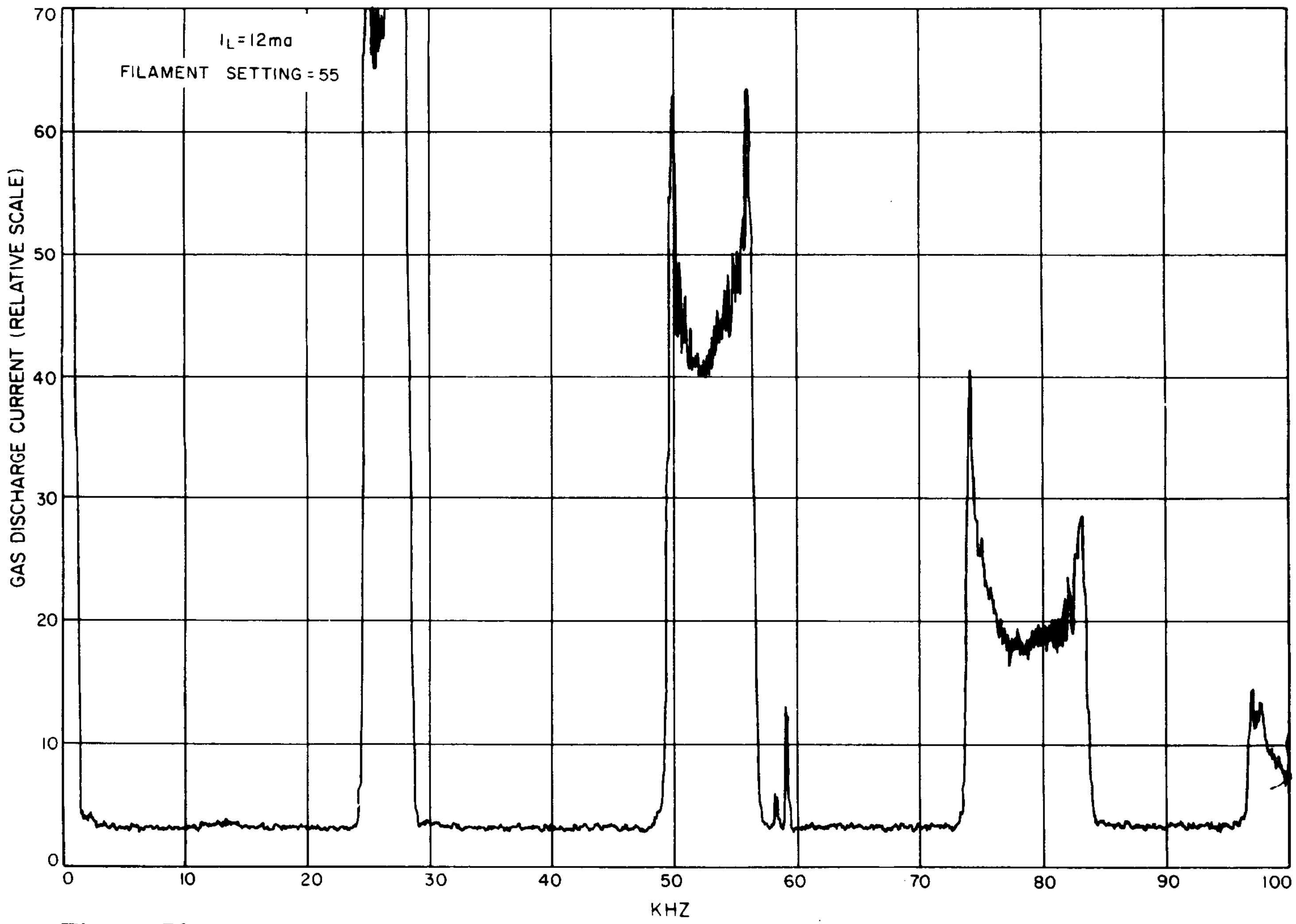

Figure 7f
Gas discharge current spectrum

PA-3-10182

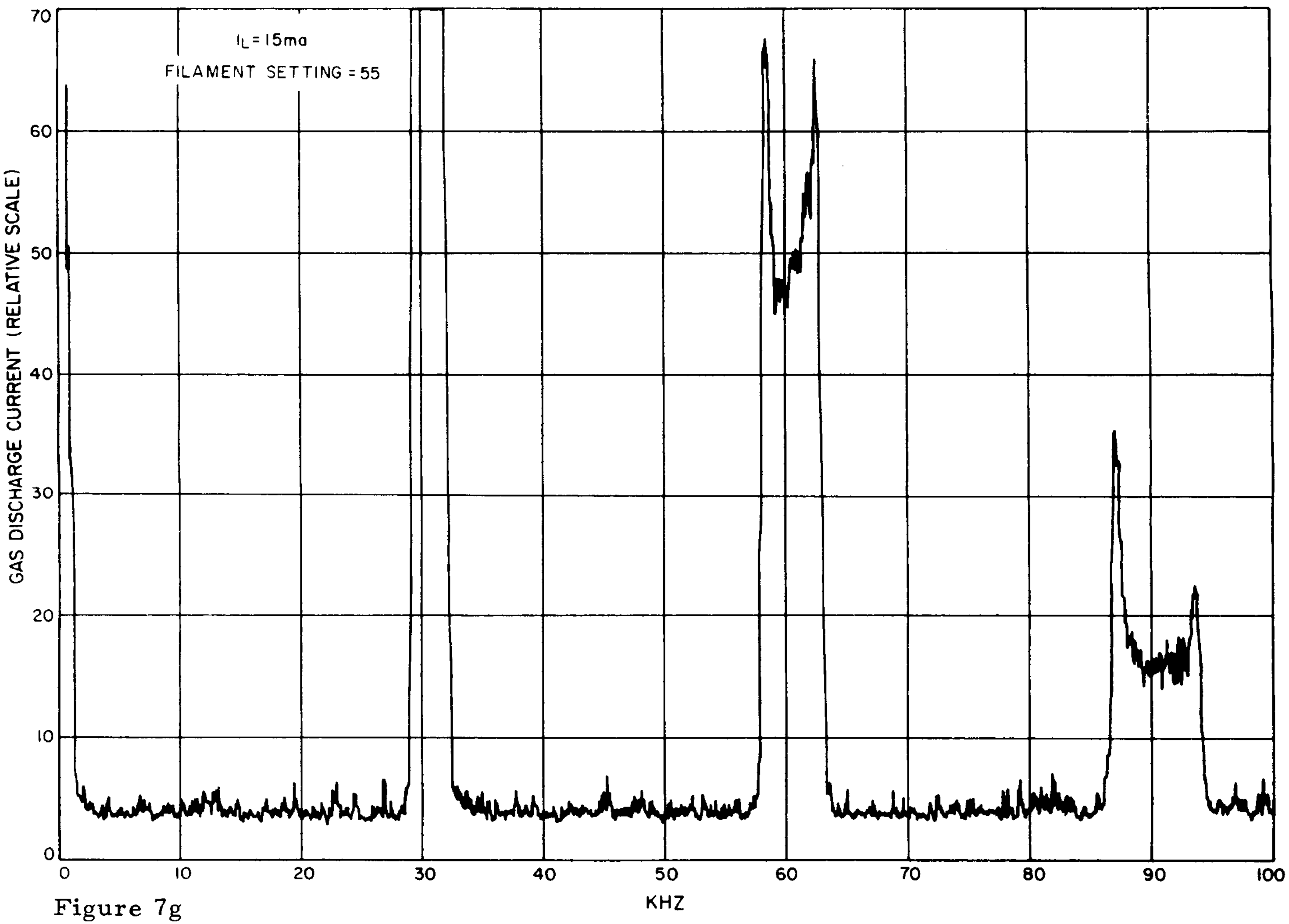

Figure 7g

Gas discharge current spectrum

PA-3-10183

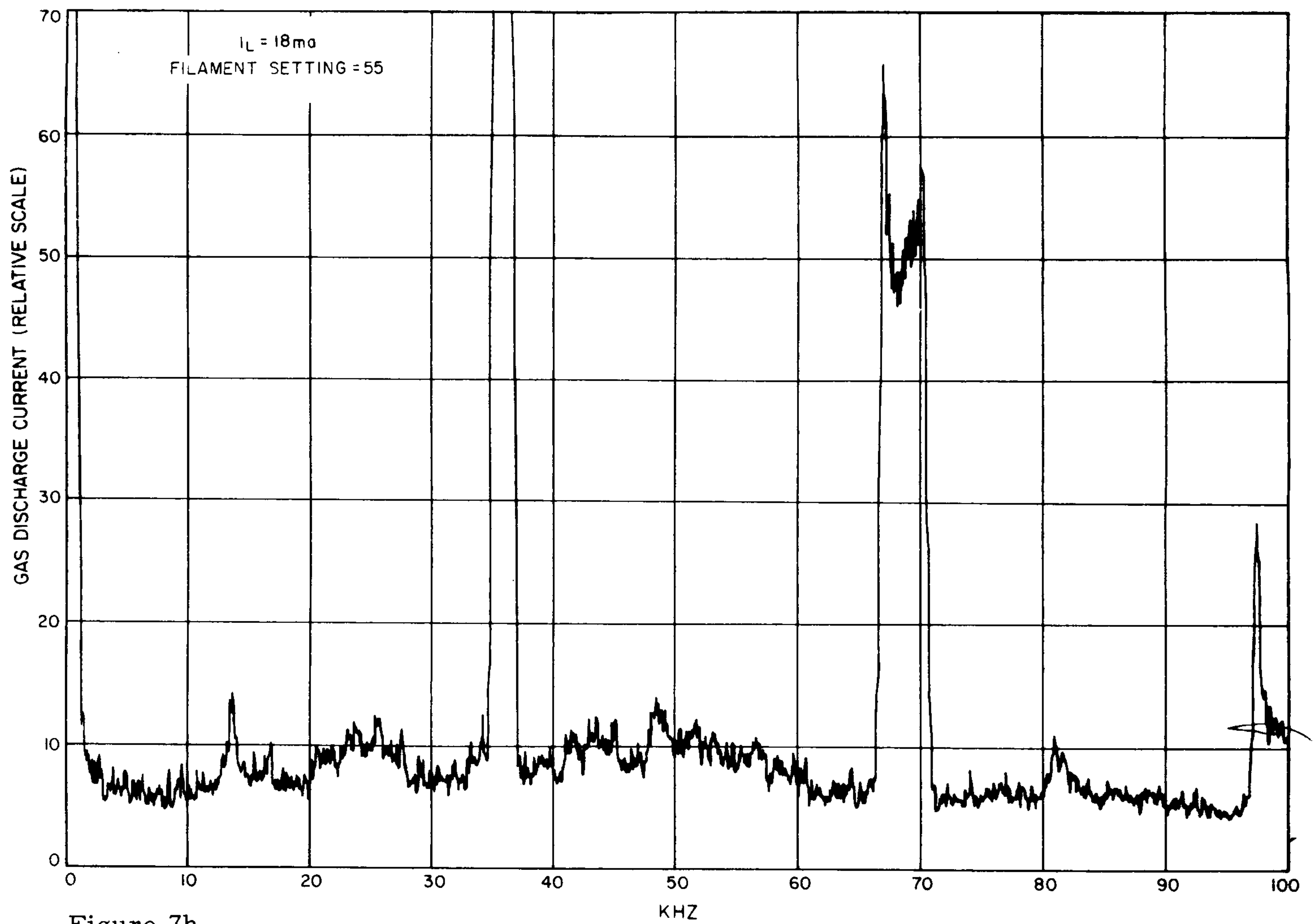

Figure 7h
Gas discharge current spectrum

PA-3-10184

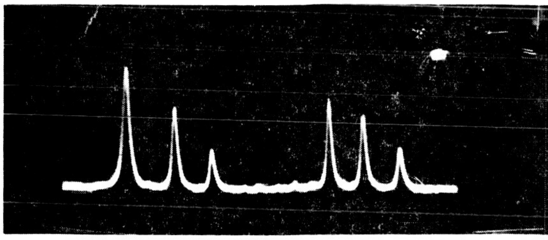

Figure 8a

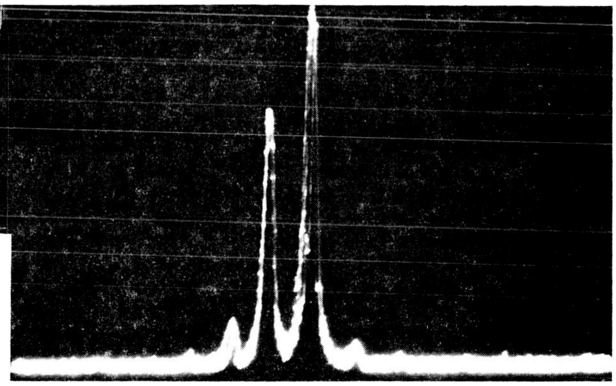

Figure 9a

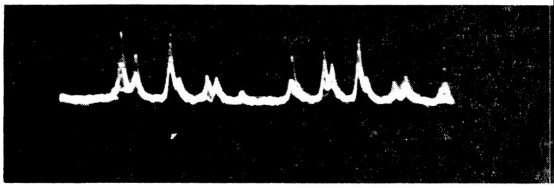

Figure 8b

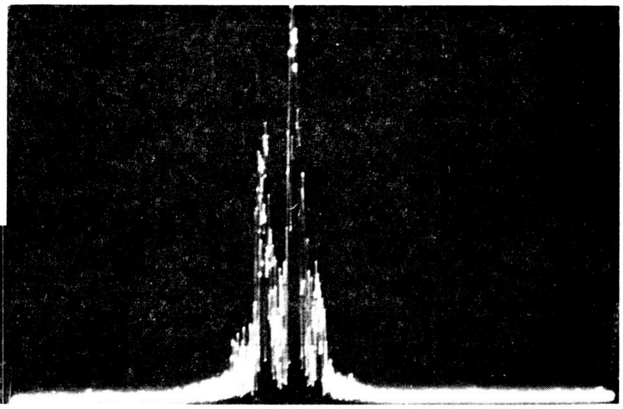

Figure 9b

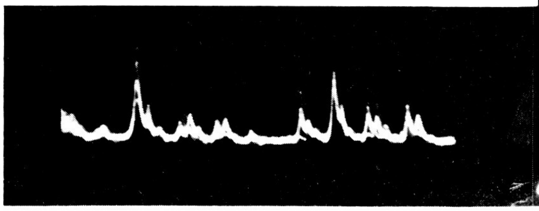

Figure 8c

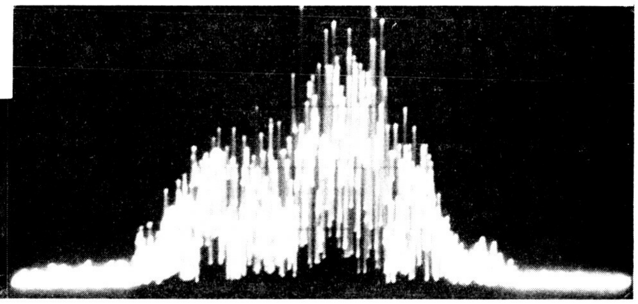

Figure 9c

Figure 8
Scanning interferance display of locked and unlocked modes

Figure 9
RF spectrum beat display under locked and unlocked conditions

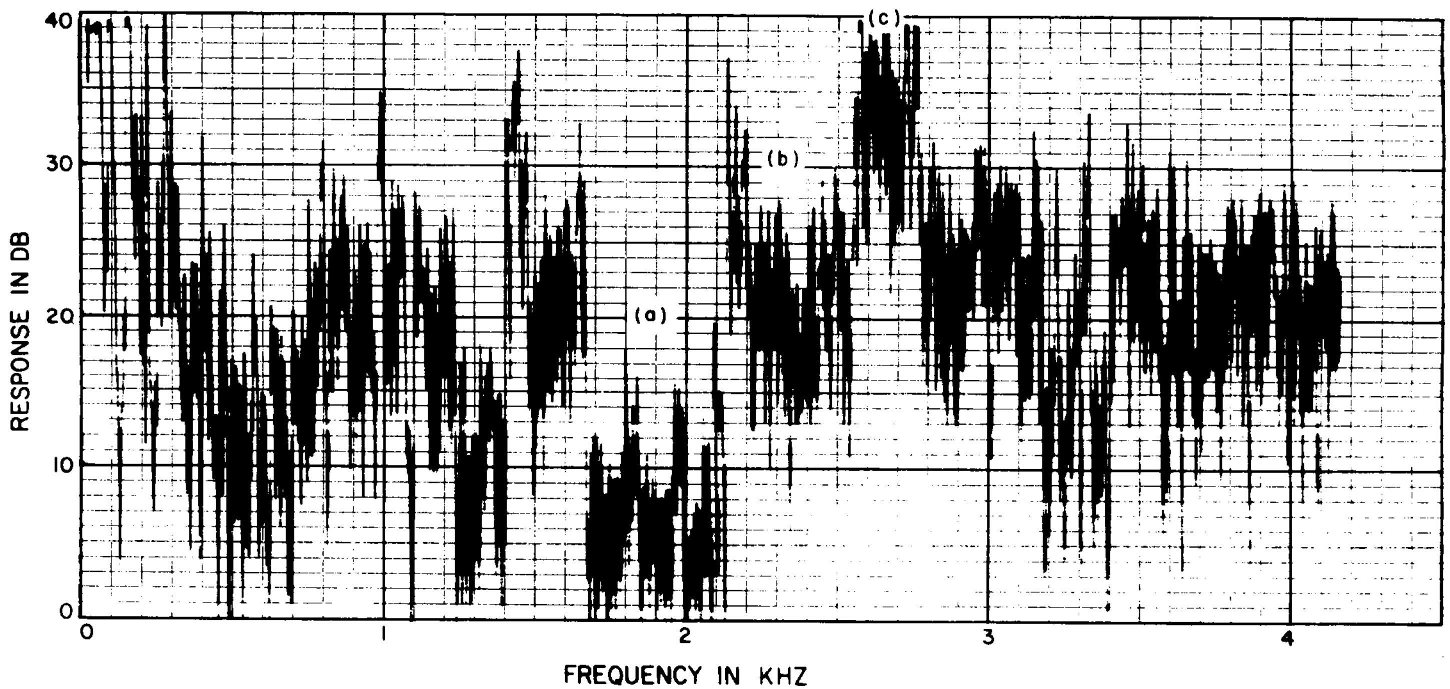

Figure 10

Photocurrent spectrum mode locking and unlocking at 1 HZ rate

PA-3-10185

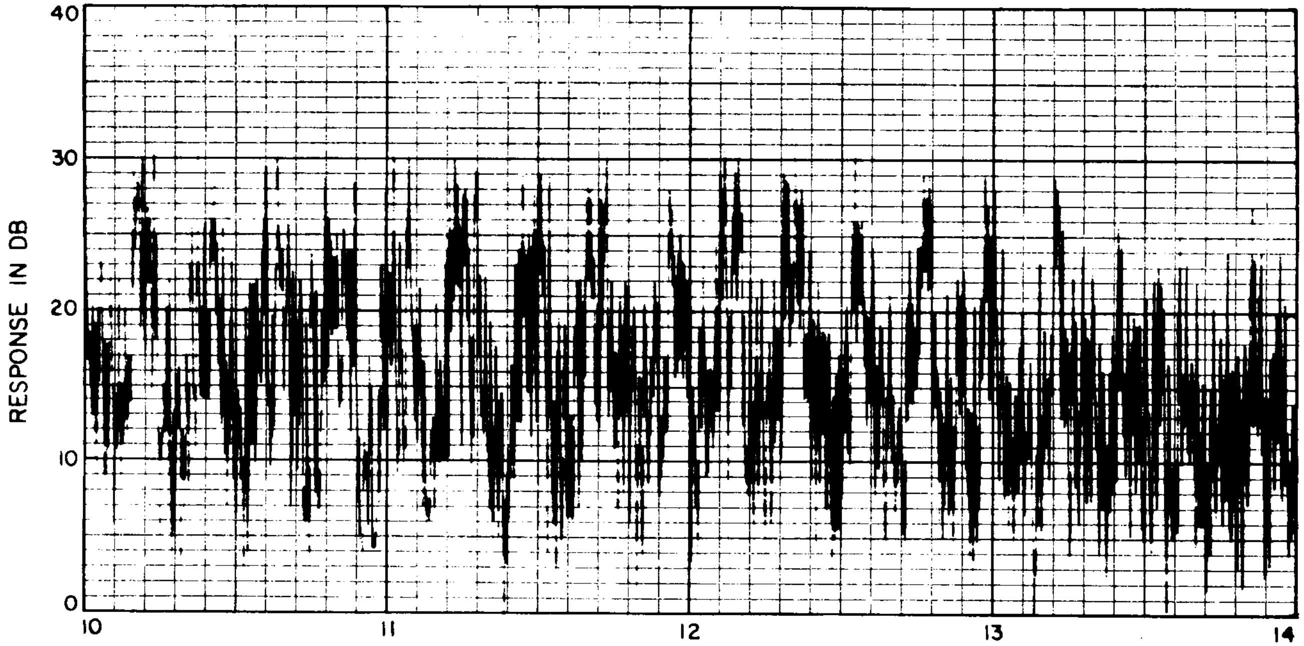

Figure 11

Photocurrent spectrum mode locking and unlocking at 1 HZ rate

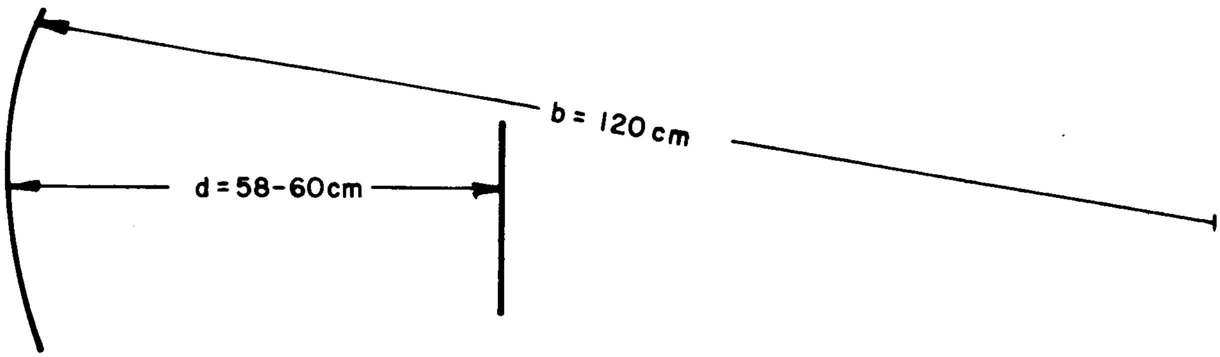

Figure 12a
Laser cavity geometry

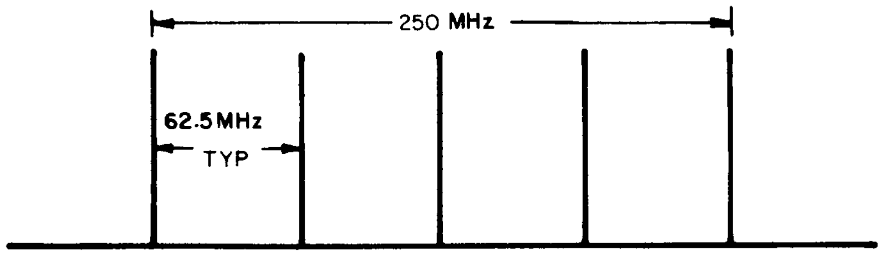

Figure 12b
Mode display for degenerate case (δ = 0)

Figure 12c
Mode display for nondegenerate case ($\delta \neq 0$)

PA-3-10187

6. REFERENCES

1. Hodara, H., and George, N., "Excess Photon Noise in Multimode Lasers," IEEE Journal of Quantum Electronics, September 1966

2. Donahue, T., and Dieke, G. H., "Oscillatory Phenomena in Direct Current Glow Discharges," Physical Review, Vol. 81, No. 2, January 15, 1951, p. 248

3. Prescott, L. J., and Van Der Ziel, A., "Gas Discharge Modulation Noise in He-Ne Laser," IEEE Journal of Quantum Electronics, Vol. QE-2, No. 7, July 1966, p. 173

4. Kubo, V., Kawabe, K., and Inuishi, Y., "Effect of Plasma Fluctuations on Gas Noise Laser," Japanese Journal of Applied Physics, Vol. 5, 1966, p. 731

5. Garscadden, A., Bletzinger, P., and Friar, E. M., "Moving Striations in a He-Ne Laser," Journal of Applied Physics, Vol. 35, No. 12, December 1964, p. 3432

6. George, N., "Improved Population Inversion in Gaseous Lasers," Proc. of the IEEE, Vol. 51, No. 8, August 1963, p. 1152

7. Crawford, F. W. and Kino, G. S., "Oscillations and Noise in Low-Pressure DC Discharges," Proc. of the IRE, Vol. 49, No. 12, December 1961, p. 1767

8. Robertson, H. S., "Moving Striations in Direct Current Glow Discharge," Physical Review, Vol. 105, No. 2, January 1957, p. 368

9. Wojaczek, K., "Simple Diffusion Theory of Moving Striations," Annalen der Physik, Vol. 3, No. 7, 1959, p. 38

10. Pekarek, L., "Theory of Moving Striations," Physical Review, Vol. 108, No. 6, December 1957, p. 1371

11. Boyd, G. D., and Kogelnick, H., "Generalized Confocal Resonator Theory," The Bell System Technical Journal, July 1962, p. 1347

12. Harding, G. O., and Li, Tingye, "Effect of Mode Degeneracy of an Output of Gaseous Optical Masers," Journal of Applied Physics, Vol. 35, No. 3, Part I, May 1964, p. 475

13. Hakeem, M. A. and Robertson, H. S., "Alkali Vapor Plasmas," Journal of Applied Physics, Vol. 31, No. 11, November 1960, p. 2063

APPENDIX

EXCESS PHOTON NOISE IN MULTIMODE LASERS

1A3—Excess Photon Noise in Multimode Lasers

H. HODARA, SENIOR MEMBER, IEEE, AND N. GEORGE, SENIOR MEMBER, IEEE

Abstract—**A theory is developed for the excess photon noise in the detected photocurrent of the multimode laser. Two simple cases are treated: in one, the modes are uncoupled and in the other, they are phase locked. Both cases can be realized when a gas laser is operated under saturation conditions well above threshold, where complicated mode interactions make a detailed analysis difficult. As predicted, the excess photon noise is zero dB, within experimental error, for the phase-locked case; and it is approximately 20 ± 3dB for a stable vibration isolated laser operating in a multimode, nonlocked condition. Precautions have been taken to eliminate extraneous noise due to power supply ripple and the like, and the highly nonideal contribution of the photomultiplier has been subtracted out.**

Introduction

The subject of fluctuations in laser beams has received a good deal of attention in recent years [1]–[4], partly because it brings out some of the fundamental differences between incoherent and coherent radiation, and partly due to some of its far reaching consequences in practical applications.

As is well known and successfully demonstrated in the Hanbury Brown and Twiss [5] and the Forester et al. [6] experiments, the fluctuations in photodetected incoherent light are made up of two distinct contributions: shot noise and wave interaction or excess photon noise. The first is inherent to the quantum nature of radiation, and the second is interpreted as beats between the randomly phased Fourier components that compose the radiation linewidth. In those experiments, the excess photon noise was several orders of magnitude below the shot noise because the degeneracy parameter [7] (average number of photons in the same quantum state) for these source temperatures[1] is much smaller than unity for incoherent light.

In the single-mode amplitude stabilized gas laser operated well above threshold the situation is markedly different. Here the degeneracy parameter exceeds unity by several orders of magnitude. Yet, excess photon noise is negligible compared to shot noise since the Fourier components composing the radiation are not randomly phased.

In multimode operation with unlocked phases, the modes beat randomly against each other, giving rise to significant additional fluctuations over the shot noise in the photodetected current. These fluctuations are interpreted as wave interaction or excess photon noise. We report in the following experiments on multimode gas lasers operated with saturated gain under phase-locked and unlocked conditions. Earlier excess noise measurements have emphasized operation in the vicinity of threshold [8], [9].

As a preliminary, we first make some pertinent remarks concerning the theory leading to the prediction of this type of noise.

Theoretical Remarks

In order to understand how modes with unlocked phase give rise to a spectrum of fluctuations, consider a simple model of two equi-amplitude stabilized modes with random phases and equal spectral width $\Delta\omega$. The expression for the instantaneous electric field is of the form

$$x_t = e^{i(\omega_1 t + \phi_{1t})} + e^{i(\omega_2 t + \phi_{2t})}. \tag{1}$$

ω_1 and ω_2 are the mode center frequencies; ϕ_{1t} and ϕ_{2t} are the respective randomly varying phase. The subscript denotes time dependence. The photodetector "sees" the square modulus of the electric field:

$$y_t = x_t x_t^* = 2\{1 + \cos(\Omega t + \psi_t)\}. \tag{2}$$

$\Omega = \omega_2 - \omega_1$ is the beat frequency, $\psi_t = \phi_{2t} - \phi_{1t}$, and the star denotes complex conjugation. In order to obtain the spectrum of the resultant photocurrent, we first calculate the autocorrelation function of y_t on an ensemble average basis,

$$\begin{aligned}\langle y_t y_{t+\tau}\rangle = 4\Big\{1 &+ \tfrac{1}{2}\langle\cos(\Omega\tau + \psi_{t+\tau} - \psi_t)\rangle \\ &+ \langle\cos(\Omega t + \psi_t)\rangle + \langle\cos[\Omega(t+\tau) + \psi_{t+\tau}]\rangle \\ &+ \frac{1}{2}\left\langle\cos\left[2\Omega\left(t + \frac{\tau}{2}\right) + \psi_{t+\tau} + \psi_t\right]\right\rangle\Big\}.\end{aligned} \tag{3}$$

If ϕ_{1t} and ϕ_{2t} have uniform probability density over the range 2π, it is readily shown that ψ_t and $\psi_{t+\tau}$ have also the same statistics, so that $\langle\cos(\Omega t + \psi_t)\rangle = \langle\cos[\Omega(t+\tau) + \psi_t]\rangle = 0$. Even in the case where ψ_t varies at approximately the same rate as Ω, one can show that the sum $\psi_{t+\tau} + \psi_t$ also has uniform probability density, thus making the last term in (3) also zero. For a time stationary process, $\langle\psi_{t+\tau} - \psi_t\rangle$ is time independent. Denoting the difference by ψ_τ, (3) reduces to

$$\langle y_t y_{t+\tau}\rangle = 4\{1 + \tfrac{1}{2}\langle\cos(\Omega\tau + \psi_\tau)\rangle\} \tag{4}$$

where

$$\langle\cos(\Omega\tau + \psi_\tau)\rangle = \int_{\substack{\text{suitable}\\ \text{limits}}} \cos(\Omega\tau + \psi_\tau)p(\psi_\tau)\,d\psi_\tau. \tag{5}$$

Manuscript received May 5, 1966; revised July 6, 1966. This paper was supported by LRC-NAS1-6003 and AFOSR-AF49 (638)-1322. This paper was presented at the 1966 International Quantum Electronics Conference, Phoenix, Ariz.

H. Hodara is with Tetra Tech, Inc., Pasadena, Calif.
N. George is with the California Institute of Technology, Pasadena, Calif.

[1] For black bodies, the average number of photons in a quantum state increases with temperature according to $1/(e^{h\nu/kT} - 1)$.

Intuitively, we expect the probability density $p(\psi_\tau)$ to be intimately tied to the joint probability $p(\psi_t, \psi_{t+\tau})$, since the latter determines the spectral power density via its Fourier transform, the autocorrelation function. The spectrum width, in turn, limits the rate at which ψ_τ can vary. This is illustrated in Fig. 1, which shows that the slope of ψ_τ cannot exceed in absolute value the half linewidth of $\Delta\omega$ of the resultant beat spectrum. At any instant, τ, $p(\psi_\tau)$ can be approximated by a Gaussian distribution with variance $\langle\psi_\tau^2\rangle$, dependent on τ. This is easily proved as follows. We assume that the slope of ψ_τ changes positively or negatively at every coherence interval $\tau_c = 1/2\Delta\omega$ with probability $q = \frac{1}{2}$ (see Fig. 1b). At a time interval τ (say $4\tau_c$), the probability of ψ_τ taking discrete values between the two slopes follows a binomial distribution. The relative occurrence of the events is indicated by the fractional numbers shown in the figure and in the corresponding histogram. The number of events is approximately $n = |\tau|/\tau_c$, as seen from the geometry of the figure. The binomial distribution variance is given by $\sigma^2 = nq = n/2$ (since $q = \frac{1}{2}$). As n grows larger the binomial distribution becomes Gaussian,

$$p(\psi_\tau) = \frac{e^{-\psi^2/2\sigma^2}}{\sigma\sqrt{2\pi}} \tag{6}$$

with

$$\frac{n}{2} = \sigma^2 = \langle\psi_\tau^2\rangle = \frac{|\tau|}{2\tau_c}. \tag{7}$$

Substituting (7) and (6) in (5) yields

$$\langle\cos(\Omega\tau + \psi)\rangle = \cos\Omega\tau\, e^{-|\tau|/4\tau_c}. \tag{8}$$

The spectral power density of the photocurrent is the Fourier transform of the autocorrelation, $\langle y_t y_{t+\tau}\rangle$,

$$S_I(\omega) = \int_{-\infty}^{\infty} \langle y_\tau y_{\tau+\tau}\rangle e^{i\omega\tau}\, d\tau \tag{9}$$

which gives, except for a normalizing factor, after substituting $\tau_c = 1/2\Delta\omega$,

$$S_I(\omega) = \delta(\omega) + \frac{(2/\Delta\omega)}{1 + \left[\dfrac{(\omega \pm \Omega)}{\Delta\omega/2}\right]^2}. \tag{10}$$

The first term is the average photocurrent (dc component). The other two terms $\pm$ are Lorentzian[2] spectra of width $\Delta\omega$ centered at Ω and $-\Omega$ (Fig. 2).

The preceding analysis, being strictly classical, yields only the spectral density fluctuation due to beats between the two randomly phased modes. The shot noise contribution does not show up in this analysis. Had the modes been phase locked, then, at any instant, the phase difference $\phi_{1t} - \phi_{2t} = \psi_0$ would be constant. The expression for the spectral current density would differ from (8) by the absence of the weighting function $e^{-|\tau|/4\tau_c}$ and the resultant photocurrent spectrum would exhibit no noise, only spikes (delta functions) centered at $\pm\Omega$.

[2] The exact spectrum can also be derived using Middleton's approach. (See D. Middleton, *Introduction to Statistical Communication Theory*. New York: McGraw-Hill, 1960, ch. 14.) The resultant autocorrelation is

$$\langle y_t y_{t+\tau}\rangle \sim 2 + \cos\Omega\tau \exp\left\{-\frac{\Delta\omega\tau^2}{2}\int s_\omega(\omega)\left(\frac{\sin\omega\tau/2}{\omega\tau/2}\right)^2 d\omega\right\}$$

where $s_\omega(\omega)$ is the normalized spectral frequency power density.

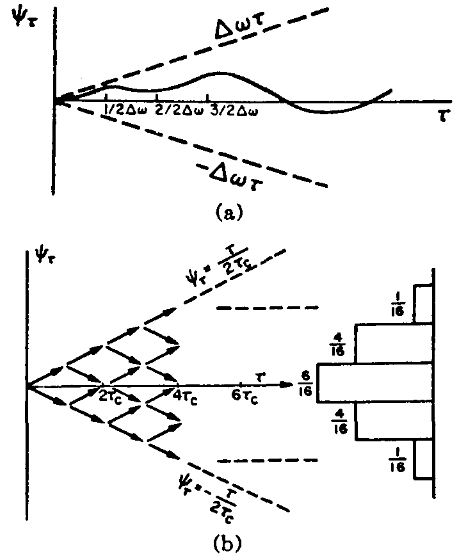

Fig. 1. (a) Member of the ensemble. (b) Probability distribution.

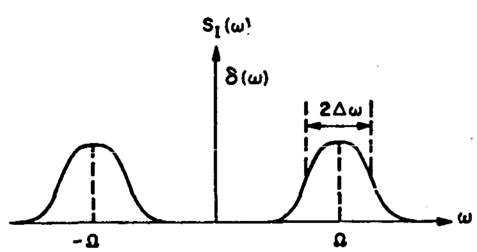

Fig. 2. Spectrum of photocurrent fluctuations for two uncoupled laser modes.

In the preceding analysis we have simplified the assumptions leading to the spectral current density. In practice, the spectrum is more likely to be Gaussian. As shown in Fig. 3, the general conclusions are still valid. In this figure we have illustrated a practical situation and emphasized the differences between the conditions leading to the presence or absence of photon noise.

In Fig. 3(a), the linewidth of a single mode centered at an optical frequency ν_0 is interpreted, in the language of communication theory, as being due to either random amplitude modulation or random frequency modulation and, in general, to a combination of both. For random FM, (1) applies with only $x_t = e^{i(\omega_1 t + \phi_{1t})}$. It follows [see Fig. 3(a)] that no beat or wave interaction noise occurs; only shot noise is present.

For random AM, (1) is modified by a random amplitude term and

$$\chi_t = A_t e^{i(\omega_1 t + \phi_1)} \tag{11}$$

it is easily proved that the photodetected current exhibits a spectrum of fluctuations due to wave interaction which lead to excess noise as indicated in Fig. 3(a).

If two modes are present, two distinct situations occur

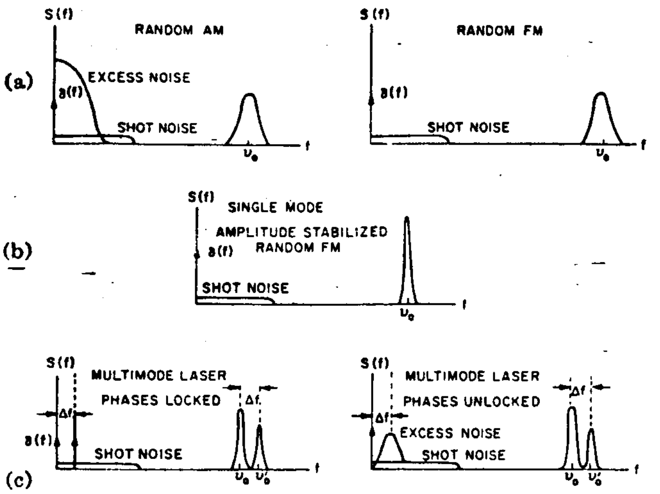

Fig. 3. Spectra of optical signal and resultant photocurrent: (a) Single-mode comparison of random AM and FM. (b) Amplitude stabilized single-mode laser. (c) Multimode laser.

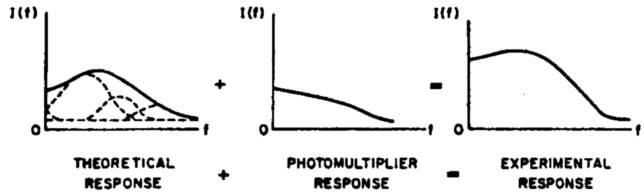

Fig. 4. Laser with uncoupled multiple modes.

depending on whether the mode phases are locked or unlocked. For purposes of analysis, the single modes are assumed to be amplitude stabilized due to saturation effects; their spectral width is attributed to random FM and it gives rise to just shot noise in the photocurrent [see Fig. 3(b)].

In the unlocked case, one visualizes each mode as having a spectrum created by two monochromatic lines traveling back and forth in a random fashion about ν_0 and ν_0', respectively. In the second case, the phases of the two modes are locked; the two lines move about randomly within their respective mode width while maintaining a constant beat frequency difference Δf. Although the beat frequency is theoretically present in the photodetected current, because of its deterministic nature it does not constitute noise [Fig. 3(c)]. On the other hand, if the modes phases are unlocked, the beat frequency is not constant; it varies over a range equal to the sum of the spectral widths of the modes and is centered at the mean frequency difference Δf. The resultant spectrum shows up as additional fluctuations over the shot noise in the photo current [Fig. 3(c)]. These fluctuations constitute excess photon noise.

The present discussion has so far been limited to two modes. In the experiment to be described, several modes are present, e.g., principal cavity modes, combination tones, and at times the closely spaced sidebands which are due to modulation by plasma oscillations [10]. The resultant excess noise, when superimposed on the photomultiplier noise, yields the expected photocurrent fluctuations shown in Fig. 4.

Measurements

In the noise measurements to be described, the 6328-Å output of a helium-neon laser is coupled simultaneously into two spectrum analyzers. One is a 0 to 50 kHz display consisting of an RCA 7102-S1 photomultiplier terminated by 100 kΩ and coupled into a General Radio Type 1900A-1521B Wave Analyzer and Recorder combination; the other is an RF display at the longitudinal beat frequency, approximately 260 MHz, consisting of a Philco Type L4501 photomixer diode coupled into an HP Type 8551-851 Spectrum Analyzer.

The laser tube is mounted in a very rigid U-shaped steel frame about 3/16 inches thick, and the entire optical apparatus is vibration isolated from the floor of the building by 30 dB over the measured range of frequencies from 1 c/s to 20 kHz. A constant current electronically regulated dc power supply is used for both anode and filament. The ripple component of the current is kept below 0.1 percent. As is customary, a resistor (150 kΩ) is located close to the anode to suppress parasitic oscillations. The discharge current *fluctuations* were measured and found uniform over the 0 to 50 kHz frequency range of interest. In addition, the light glow from the side walls of the discharge tube was photodetected and the resulting current was found to be shot noise limited. However, low frequency plasma oscillations could be induced by lowering the cathode temperature, thereby decreasing the space charge region. The low frequency *tones* with their associated sidebands previously reported by Y. Inuishi and T. Uchida are then observed in the laser output, the discharge current, and the sidewall light.

Vibrations of components due to air movements were reduced below observable levels by enclosing these parts in felt-lined shields. Short enclosed optical paths were used to keep air-motion induced signal fluctuations negligible. The laser is operated in saturation condition at a constant output power of 3 mW for all of the measurements reported. Two different modes of operation are observed: phase-locked and uncoupled modes.

Phase-Locked Modes

This mode is characterized by the appearance of stable equispaced beats as shown in the RF spectrum analyzer display of Fig. 5. The low-frequency spectral noise does not vary appreciably with the number of beats under phase-locked conditions nor does it change markedly when low frequency plasma oscillations are induced, except for the appearance of the previously mentioned beats which are not plotted as noise. The corresponding low-frequency spectral noise record is shown in Curve (1) of Fig. 6 for any of the cases of Fig. 5(a), (b), or (c). In order to compare this level to the shot noise limited output, an incandescent lamp powered with a dc supply is used to establish the "white light" noise level. The low-frequency noise spectrum (Curve (2) of Fig. 6) due to this incandescent source is measured at the same value (8 μA) of dc photocurrent which is used

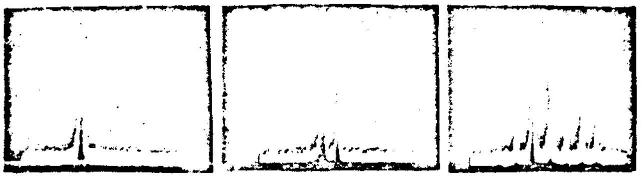

(a) (b) (c)

Fig. 5. Spectrum display of beats centered at 260 MHz with 300 kHz width for coupled modes. (a) One beat. (b) Two beats. (c) Seven beats.

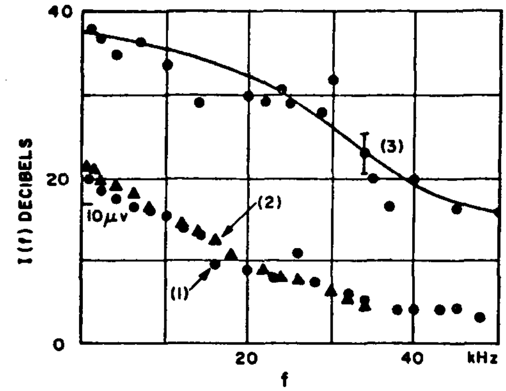

Fig. 6. Low-frequency noise spectrum for (1) coupled modes, (2) shot noise level, and (3) uncoupled modes showing excess photon noise.

Fig. 7. Spectrum display of beats for uncoupled modes (260 MHz, with display width of 300 kHz).

in the laser tests. Comparison of Curves (1) and (2) shows that for phase-locked operation the detected photomultiplier noise is equal to the measured white light noise within the limits of experimental error, ± 2 dB. It is interesting to note that the level of noise for the photomultiplier in the 0 to 50 kHz band is typically far above the shot nose value $(2eI_0\Delta f)^{1/2}$ for operating currents of 8 μA. In our experiments, the level was 20 times (or about 30 dB) higher than the theoretical level below 10 kHz, and it approached the shot noise level beyond 50 kHz.

The white light is a practical means of establishing this reference for experimental purposes, but in applications it would be desirable to eliminate this effect.

Uncoupled Modes

Although the phase-locked condition could be maintained for periods of time in excess of a half hour, which was adequate for our measurements, this condition is relatively unstable. These instabilities can arise or be induced by some external fluctuation, e.g., vibration of a mirror or surge of the power supply; or, they may possibly be due to frequency pulling interactions. In order to induce the uncoupled case in a fairly regular manner, we scanned one mirror of the laser cavity longitudinally at a rate of 0.1 Hz. Typically, the laser is observed to go through a fairly regular sequence of mode patterns (Fig. 5) indicating cyclic frequency pulling interactions [11]–[13]. This is followed by a period of instability during which the modes are uncoupled (Fig. 7) and characterized by excess photon noise as shown in the low-frequency spectral record, Curve (3) of Fig. 6. As seen from this curve, the excess photon noise for the uncoupled mode condition is characteristically 20 ± 3 dB over the frequency range from 0 to 50 kHz.

Summary

The excess photon noise for a multimode laser operating far above threshold has been measured, and it is found that mode interaction instabilities may give rise to an excess level of 20 ± 3 dB over the frequency range from 0 to 50 kHz. Either in single-mode operation or when the modes are phase locked, it is found that the level of excess photon noise is zero within the limits of the experimental error. Both results are in accord with the theory presented here for the simplified two mode case.

The source fluctuations inherent in the unlocked multimode laser must be accounted for or eliminated in practical applications such as studies of propagation through atmospheric turbulence or in certain laser communication links.

Acknowledgment

We acknowledge helpful discussions with D. H. Close, D. McIver, J. Matthews, R. J. Marquedant, and J. Yoh. We are also indebted to Prof. L. Mandel for reading the manuscripts and suggesting improvements.

References

[1] P. T. Bolwijin, C. T. J. Alkemade, and G. A. Goschloo, "Excess photon noise and spectral line shape of laser beam," *Phys. Letters (The Netherlands)*, vol. 4, p. 59, March 1963.
[2] Charles Freed and H. A. Haus, "Measurement of amplitude noise in optical cavity masers," *Appl. Phys. Letters*, vol. 6, p. 85, March 1, 1965.
[3] J. A. Armstrong and A. W. Smith, "Intensity fluctuations in GaAs laser," *Phys. Rev. Letters*, vol. 15, p. 65, January 18, 1965.
[4] H. Hodara, "Statistics of thermal and laser radiation," *Proc. IEEE*, vol. 53, pp. 696–704, July 1965.
[5] R. Hanbury Brown and R. Q. Twiss, "Interferometry of the intensity fluctuations in light," *Proc. Roy. Soc.*, vol. A242, p. 300, 1957.
[6] A. T. Forrester, R. A. Gudmundsen, and P. O. Johnson, "Photoelectric mixing of incoherent light," *Phys. Rev.*, vol. 99, p. 1961, 1955.
[7] L. Mandel, "Photon degeneracy in light from optical masers and other sources," *J. Opt. Soc. Am.*, vol. 51, p. 797, 1961.
[8] J. A. Bellisio, C. Freed, and H. A. Haus, "Noise measurements on He-Ne laser oscillators," *Appl. Phys. Letters*, vol. 4, p. 5, January 1, 1964.
[9] A. W. Smith and J. A. Armstrong, "Observation of photon counting distribution for laser light below threshold," *Phys. Letters*, vol. 19, p. 650, January 1, 1966.
[10] F. W. Crawford and G. S. Kino, "Oscillations and noise in low-pressure dc discharges," Proc. IRE, vol. 49, pp. 1767–1788, December 1961.
[11] W. E. Lamb, Jr., "Theory of an optical maser," *Phys. Rev.*, vol. 134, p. A1429, June 15, 1964.
[12] D. H. Close, "Nonlinear effects in traveling wave laser amplifiers," AFOSR Rept. 65-0999, May 1965.
[13] J. Haisma and G. Bouwhuis, "Mode competition and combination tones in a gas laser," *Phys. Rev. Letters*, March 1965.